ACKNOWLEDGMENTS

This study was supported by the Health and Labour Sciences Research Grants of Research on Intractable Diseases from the Ministry of Health, Labour and Welfare, Tokyo, Japan.

REFERENCES

Aramaki M, Udaka T, Kosaki R, Makita Y, Okamoto N, Yoshihashi H, Oki H, Nanao K, Moriyama N, Oku S, Hasegawa T, Takahashi T, Fukushima Y, Kawame H, Kosaki K. 2006a. Phenotypic spectrum of CHARGE syndrome with CDH7 mutations. J Pediatr 148:410–414.

Aramaki M, Udaka T, Torii C, Samejima H, Kosaki R, Takahashi T, Kosaki K. 2006b. Screening for CHARGE syndrome mutations in the CDH7 gene using denaturing high-performance liquid chromatography. Genet Test 10:244–251.

Blake KD, Davenport SL, Hall BD, Hefner MA, Pagon RA, Williams MS, Lin AE, Graham JM Jr. 1998. CHARGE association: An update and review for the primary pediatrician. Clin Pediatr (Phila) 37:159–173.

Cohen J. 1960. A coefficient of agreement for nominal scales. Educ Psychol Meat 20:37–46.

Holak HM, Kohlhase J, Holak SA, Holak NH. 2008. New recognized ophthalmic morphologic anomalies in CHARGE syndrome caused by the R2319C mutation in the CHD7 gene. Ophthalmic Genet 29:79–84.

Hornby SJ, Adolph S, Girbert CE, Dandona L, Foster A. 2000. Visual acuity in children with coloboma. Clinical features and a new phenotypic classification system. Ophthalmology 107:511–520.

Jongmans MC, Admiraal RJ, van der Donk KP, Vissers LE, Baas AF, Kapusta L, van Hagen JM, Donnai D, de Ravel TJ, Veltman JA, van Kessel AG, De Vries BB, Brunnaer HG, Hoefsloot LH, van Ravenswaaj CM. 2006. CHARGE syndrome: The phenotypic spectrum of mutations in the CHD7 gene. J Med Genet 43:306–314.

Lalani SR, Saliullah AM, Fernbach SD, Harutyunyan KG, Thaller C, Peterson LE, McPherson JD, Gibbs RA, White LD, Hefner M, Davenport SLH, Graham JM Jr, Bacino CA, Glass NL, Towbin JA, Craigen WJ, Neish SR, Lin AE, Belmont JW. 2006. Spectrum of CHD7 mutations in 110 individuals with CHARGE syndrome and genotype–phenotype correlation. Am J Hum Genet 78:303–314.

Landis JR, Koch GG. 1977. The measurement of observer agreement for categorical data. Biometrics 33:159–174.

Pagon RA, Graham JM Jr, Zonana J, Yong SL. 1981. Coloboma, congenital heart disease, and choanal atresia with multiple anomalies: CHARGE association. J Pediatr 99:223–227.

Russell-Eggitt IM, Blake KD, Taylor DSI, Wyse RKH. 1990. The eye in the CHARGE association. Br J Ophthalmol 74:421–426.

Vissers LE, van Ravenswaaij CM, Admiraal R, Hurst JA, de Vries BB, Janssen IM, van der Vliet WA, Huys EH, de Jong PJ, Hamel BC, Schoenmakers EF, Brunner HG, Veltman JA, van Kessel AG. 2004. Mutations in a new member of the chromodomain gene family cause CHARGE syndrome. Nat Genet 36:955–957.

World Health Oraganization. 1992. International statistical classification of diseases and related problems. 10th revision. Vol. 1. Geneva, Switzerland: World Health Organization.

Zentner GE, Layman WS, Martin DM, Scacheri PC. 2010. Molecular and phenotypic aspects of CHD7 mutation in CHARGE syndrome. Am J Med Genet Part A 152A:674–686.

Clinical Features of Anterior Segment Dysgenesis Associated With Congenital Corneal Opacities

Chika Shigeyasu, MD, Masakazu Yamada, MD, PhD, Yoshinobu Mizuno, MD, Tadashi Yokoi, MD, Sachiko Nishina, MD, PhD, and Noriyuki Azuma, MD, PhD

Purpose: Anterior segment dysgenesis is one of the main causes of congenital corneal opacities. In this study, we investigated the clinical features and visual outcomes of patients with anterior segment dysgenesis in a large number of cases.

Methods: The medical records of patients with congenital corneal opacities in relation to anterior segment dysgenesis seen in the National Center for Child Health and Development, Japan, between April 2002 and October 2009, were retrospectively studied.

Results: Records of 220 eyes of 139 patients were reviewed. Mean follow-up period was 5 years. Clinical diagnoses were Peters anomaly (72.7%), anterior staphyloma (11.4%), Rieger anomaly (7.7%), sclerocornea (6.4%), and others (1.8%). Visual acuity was measured in 61 patients. The best-corrected visual acuity in the better eye of bilaterally involved patients was 20/60 to 20/1000 (low vision according to the *International Classification of Diseases, Ninth Revision, Clinical Modification*) in 43.2% and less than 20/1000 (legally blind) in 24.3%. Fundus examination was performed in 82 eyes, and disorders were seen in 12 (12 of 82; 14.6%). Systemic abnormalities were present in 35 patients (35 of 139; 25.2%); a family history was present in 5 patients (5 of 139; 3.6%). Of the 160 eyes of 109 patients with Peters anomaly, 51 patients (51 of 109; 46.8%) had bilateral Peters anomaly, 30 (30 of 109; 27.5%) had fellow eyes that were normal, and 28 (28 of 109, 25.7%) showed other abnormal ocular findings in the fellow eye.

Conclusions: Anterior segment dysgenesis shows diverse clinical features, various severities of corneal opacities, and visual outcomes. Further understanding of the disease as an abnormality during embryogenesis and neural crest cell differentiations may be required.

Key Words: anterior segment dysgenesis, congenital anomaly, cornea, Peters anomaly, visual impairment

(*Cornea* 2012;31:293–298)

The causes of congenital corneal opacities (CCOs) are diverse. CCO can be genetic, glaucomatous, infectious, traumatic, developmental, metabolic, idiopathic, or toxic. Furthermore, these causes can also overlap.[1–3] When we consider the congenital causes, indicating that the corneal opacity exists in a neonate, one of the main causes, of CCO is anterior segment dysgenesis (ASD). A number of these cases are bilaterally involved and are also accompanied by other ocular malformations, sometimes with complex systemic diseases.[4] However, only a few reports concerning these abnormalities in series with a large number of cases are present.[1,5] This is because of the difficulty in performing an epidemiological study that samples a large number of newborns. Furthermore, making a precise diagnosis of a rare entity such as ASD is difficult.

ASD is induced by abnormalities during embryogenesis and neural crest cell differentiations.[6–13] Previously, ASD was called anterior chamber cleavage syndrome[12] or mesodermal dysgenesis of the iris and cornea.[14] Because it is now known that no development of a cleavage plane as the anterior segment forms and differentiates occurs[8] and because no mesoderm is involved,[7] these terms have been deemed inappropriate. Mutations in the ASD genes, *PAX6*, *PTX2*, *FOXC1*, *FOXE3*, and *CYP1B1*, have been identified.[15,16] Investigators have suggested various ASD classifications based on embryological contribution,[7] developmental arrest,[9] neural crest proliferation and migration patterns,[10] neural crest origin,[11] and anatomical findings.[12] ASD classification is sometimes complicated because it is not unusual that dysgenesis exists not only alone but also in combination with other disorders. In this study, we investigated the clinical features and visual outcomes of ASD-associated CCO in a large number of patients. We also reviewed the classification of ASD[3,6–13,15,17,18] and compared the diagnosis of both eyes of patients with Peters anomaly in 1 eye to study ASD overlap.[19–21]

SUBJECTS AND METHODS

We retrospectively reviewed the computerized medical records of all patients with ASD-associated CCO seen at the National Center for Child Health and Development (Tokyo, Japan) between April 1, 2002, and October 31, 2009.

Received for publication August 10, 2010; revision received November 19, 2010; accepted December 12, 2010.

From the Division for Vision Research, National Institute of Sensory Organs, National Hospital Organization Tokyo Medical Center, Tokyo, Japan; and Department of Ophthalmology, National Center for Child Health and Development, Tokyo, Japan.

Supported in part by a grant from the Ministry of Health, Labor, and Welfare, Japan.

None of the authors have any proprietary interest in any materials in this article.

Reprints: Chika Shigeyasu, Division for Vision Research, National Institute of Sensory Organs, National Hospital Organization Tokyo Medical Center, 2-5-1 Higashigaoka, Megurao-ku, Tokyo 152-8982, Japan (e-mail: shigeyasuchika@kankakuki.go.jp).

The data were collected from computerized medical records, entering the diagnosed disease name as a key word, and all the medical records were reviewed again. The adult patients who had ASD-associated CCO diagnosed when they were younger at the former National Children's Hospital (from 1965 to March 2002) who came to the National Center for Child Health and Development for the first time were also included. In this study, ASD cases without the risk of emerging CCO and congenital aniridia were excluded. We evaluated laterality, ASD type, visual outcome, location of opacity, posterior segment abnormalities, systemic diseases, family history, and clinical course of the disorder.

Laterality (unilateral or bilateral) was diagnosed only by the existence of ASD, and other ocular findings were excluded. ASD type was diagnosed by slit-lamp examination and, when possible, with the assistance of ultrasound biomicroscopy (UBM) and anterior segment optical coherence tomography (AS-OCT). Visual outcomes were measured considering the child's age and mental development. Picture tests were used for preverbal children. In older children, angular vision using Landolt rings followed by cortical vision was measured and converted to Snellen visual acuity. Corneal opacity location was categorized into 5 groups: diffuse, central, center to periphery, peripheral opacity, and other (including minimal corneal involvement and location not classifiable). Posterior segment abnormalities were diagnosed by clinical examination, using the slit lamp and funduscope, with the help of B-mode echography when the posterior segment was invisible because of CCO. Records of systemic disease and family history from interviews during the clinical course of the child's condition were reviewed. For a better understanding of ASD overlap, we analyzed diagnosis of both eyes of patients with Peters anomaly to observe differences in ASD diagnosis between the eyes.

RESULTS

Medical records of 220 eyes of 139 patients with ASD-associated CCO were reviewed. Among the patients, 68 were men (109 eyes) and 71 were women (111 eyes). Age at the first examination ranged from 0 months to 25 years (mean, 1.2 years; SD, 2.7). The mean follow-up period was 5 years (range, 0 months to 21 years).

Eighty-one patients (162 of 220 eyes; 73.6%) had bilateral corneal opacities and 58 (58 of 220 eyes; 26.4%) had unilateral ones. Clinical diagnosis was as follows: Peters anomaly in 160 eyes (72.7%), anterior staphyloma in 25 eyes (11.4%), Rieger anomaly in 17 eyes (7.7%), sclerocornea in 14 eyes (6.4%), and other (of unknown origin) in 4 eyes (1.8%) (Fig. 1).

Diagnosis was made by slit-lamp examination with UBM and AS-OCT assistance in cases of severe corneal opacity. Figure 2 shows the slit-lamp photograph and corresponding image of UBM and AS-OCT in patients with bilateral Peters anomaly. The iridocorneal angle structure can be seen in detail.

Visual acuity was measured in 98 eyes of 61 patients (37 bilateral and 24 unilateral cases). Table 1 shows the best-corrected visual acuity of the eyes in bilateral and unilateral cases, and Table 2 shows the visual acuity ranges based on the better eye. The best-corrected visual acuity in the better eye of bilaterally involved patients was lower than 20/60 (low vision

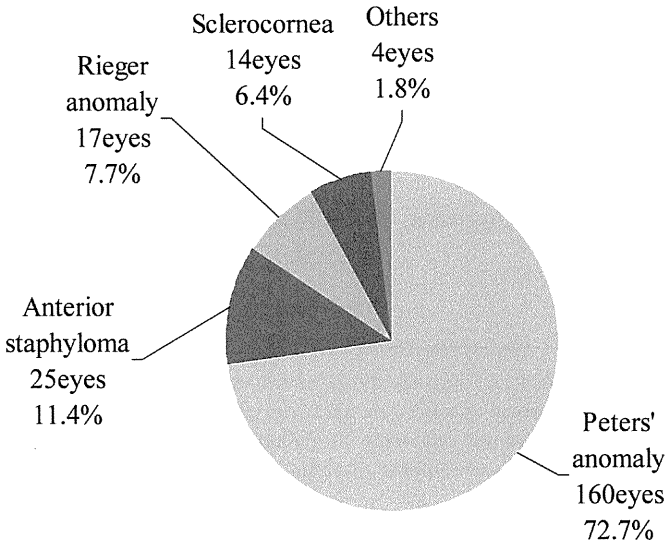

FIGURE 1. Clinical diagnosis of ASD with CCO (n = 220 eyes).

according to the *International Classification of Diseases, Ninth Revision, Clinical Modification*) in 43.2% and 20/1000 or worse (legally blind) in 24.3%. In total, 67.5% of patients with bilateral CCO had visual disability diagnosed.

Corneal opacity was diffuse in 48.6% of eyes, central in 17.7%, and peripheral and center to peripheral in approximately 10% each (Table 3). Of the 170 eyes of patients with corneal opacity whom we were able to follow-up, 142 (83.5%) showed no noticeable change and 28 (16.5%) showed a slight improvement. Improvement of the corneal opacity was mostly seen in patients with Peters anomaly.

Fundus examination was performed using the funduscope in 82 eyes, and fundus disorders were seen in 12. However, 138 eyes could not be examined by funduscope because of haziness. Among those 138 eyes, 125 were without major disorders, as examined by B-mode echography (Table 4). The most common disorders were persistent fetal vasculature in 4 eyes, followed by coloboma, chorioretinal atrophy, and optic nerve hypoplasia (Table 5).

Systemic abnormalities were present in 35 patients (25.2%). Multiple deformations, such as chromosome abnormality, hydrocephalus, polysyndactyly, and syndactylia, were seen in 16 patients, followed by cardiovascular disease in 5, neurologic disease (including brain hypoplasia, mental retardation, cerebral palsy, and seizure) in 5, craniofacial disease in 3 (cleft lip and palette, macroglossia and oral tumor, and dental hypoplasia), thyroid disease in 2, urinary disease in 2, and otologic disease (deafness and preauricular appendage) in 2 (Table 6). Axenfeld–Rieger syndrome, which is characterized by components of the ocular symptoms of Axenfeld anomaly and Rieger anomaly, and nonocular symptoms of Rieger syndrome were seen in 4 patients. There was a family history of ocular disorders in 5 patients (3.6%); 4 patients had a family history of Peters anomaly and 1 had a history of anterior staphyloma.

Of the 220 eyes of 139 patients in this study, we diagnosed Peters anomaly in 160 eyes of 109 patients. We reviewed the condition of the fellow eye among these 109

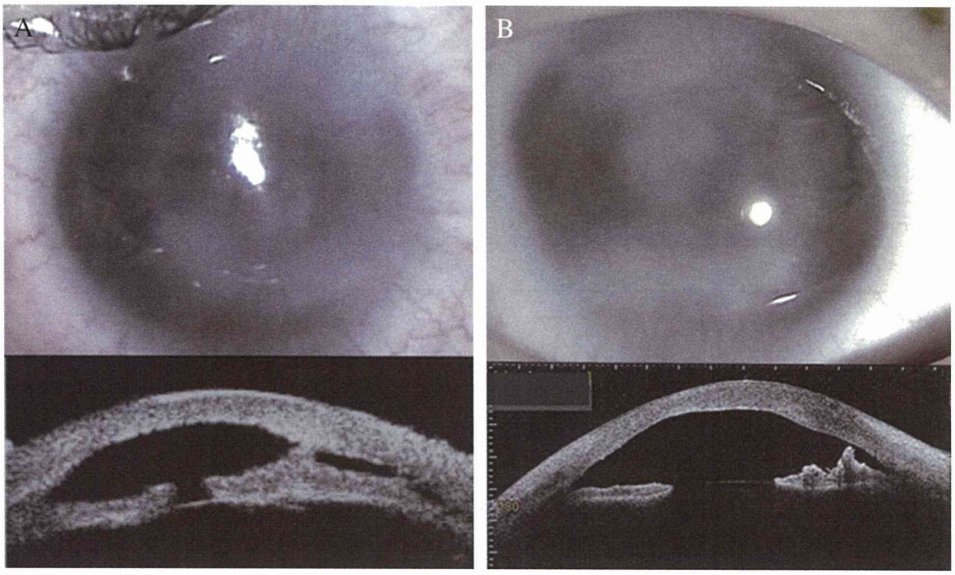

FIGURE 2. Slit-lamp photograph and corresponding image by UBM (A) and AS-OCT (B) of bilateral Peters anomaly. The iridocorneal angle can be seen more clearly in the image of AS-OCT, although there are limitations from the sclera and poor visualization of the ciliary body.

patients with Peters anomaly. Thirty patients (27.5%) had normal fellow eyes and 79 (72.5%) showed abnormal ocular findings in the fellow eye. The abnormal ocular findings were Peters anomaly in 51 eyes, anterior staphyloma in 9, sclerocornea in 6, Rieger anomaly in 5, persistent pupillary membrane in 3, macular hypoplasia in 2, and optic disc hypoplasia, high myopia, and aniridia in 1 each. Thus, within patients with ocular abnormalities in the fellow eyes of Peters anomaly, 64.6% had bilateral Peters anomaly and 93.7% had bilateral ASD. From another viewpoint, 67.9% of patients with Peters anomaly also had bilateral ASD (Fig. 3).

DISCUSSION

Ocular malformation incidence in newborns is reported to be low, from 3.3 to 6.0 per 10,000 newborns[22,23]; although extremely rare, severe ocular malformations are a lifelong vision-threatening disease. Bermejo and Martinez-Frias[5] indicate that the range in statistics emerges from a statistical bias based on samples taken from special schools or clinics and the time of data sampling. Furthermore, they also report the incidence of CCO to be 3.1 per 100,000.

Among the diverse causes of CCO, ASD stands out as the main cause at present. Furthermore, ASD incidence is rare, and our study presents the largest series of evidence assembled to date on the diagnosis of this disorder. The description of clinical features and visual outcomes for a large number of cases would be valuable for understanding the disease and a further study of the disease. Because ASD is induced by the abnormalities during embryogenesis and neural crest cell differentiations, the key to understanding ASD is to review the embryology of anterior segment. At approximately the sixth week of gestation, separation of lens vesicle and basement membrane of the surface ectoderm, which will become corneal

TABLE 1. Best-corrected Visual Acuity of Eyes of Bilateral and Unilateral Cases Based on the *International Classification of Diseases, Ninth Revision, Clinical Modification*

	Bilateral (n = 74)		Unilateral (n = 24)	
Visual Acuity	Eyes	%	Eyes	%
Near-normal vision				
Range of normal vision (>20/25)	10	13.5	3	12.5
Near-normal vision (<20/25)	4	5.4	4	16.7
Low vision				
Moderate low vision (<20/60)	12	16.2	1	4.2
Severe low vision (<20/160)	11	14.9	1	4.2
Profound low vision (<20/400)	5	6.8	2	8.3
Near-blindness				
Near-blindness (<20/1000)	23	31.1	4	16.7
Total blindness (no light perception)	9	12.2	9	37.5

n, number of eyes.

TABLE 2. Best-corrected Visual Acuity in the Better Eye Based on the *International Classification of Diseases, Ninth Revision, Clinical Modification*

	Bilateral (n = 37)		Unilateral (n = 24)	
Visual Acuity	Cases	%	Cases	%
Near-normal vision				
Range of normal vision (>20/25)	8	21.6	21	87.5
Near-normal vision (<20/25)	4	10.8	3	12.5
Low vision				
Moderate low vision (<20/60)	10	27.0	—	—
Severe low vision (<20/160)	5	13.5	—	—
Profound low vision (<20/400)	1	2.7	—	—
Near-blindness				
Near-blindness (<20/1000)	9	24.3	—	—
Total blindness (no light perception)	0	0	—	—

n, number of cases.

TABLE 3. Frequencies of Corneal Opacity Location

Opacity Location	Eyes (n = 220)	%
Diffuse	107	48.6
Center	39	17.7
Center to the periphery	24	10.9
Periphery	21	9.5
Others	29	13.2

n, number of eyes.

TABLE 5. Fundus Disorders Among Patients With ASD Examined by Funduscopy

Fundus Disorders	Eyes (n = 82)	%
Persistent fetal vasculature	4	4.9
Coloboma	3	3.7
Chorioretinal atrophy	3	3.7
Optic disc hypoplasia	2	2.4
No major disorders	70	85.4

n, number of eyes.

epithelium, occurs and is followed by 3 successful waves. The first wave gives rise to the corneal endothelium and trabecular meshwork, the second gives rise to the corneal keratocytes and corneal stroma, and the third becomes the iris. The arrest of any of these developmental stages will induce ASD.

Three-fourths of our patients showed bilateral CCO. This rate was higher than that in the previous reports from Rezende et al[1] (55.3%). We postulate that the difference emerges because of patient samples of CCO. We limited our patients to those with ASD; therefore, patients with popular unilateral CCO, such as limbal dermoid, were excluded from our study. Furthermore, because our data were from the corneal practice of a specialized children's hospital, the patient population seems to fall into the range of severe bilateral CCO.

In our study, the majority of ASD was diagnosed as Peters anomaly. Clinical features of Peters anomaly are diverse, from mild to severe. ASD is classified in detail by its characteristics, although it has a broad spectrum. Some cases overlap other conditions and therefore are impossible to classify. Rieger anomaly is classified as a mild ASD type, and sclerocornea and anterior staphyloma are classified as severe ASD types. The remaining cases will be classified in a broad range of Peters anomaly. Therefore, further understanding of ASD as a disease of abnormalities during embryogenesis and neural crest cell differentiations as a whole is required.

Visual acuity outcome was severe. Forty percent to 50% of both bilateral and unilateral eyes were less than 20/1000, and patients had legal blindness diagnosed according to the *International Classification of Diseases, Ninth Revision, Clinical Modification*. In unilateral and bilateral cases with difference in severity, deprivation of form vision occurs in the worse eye and development of vision seems to be disturbed. Classifying by the better eye, 43.2% of patients with bilateral Peters anomaly had low vision and 24.3% were legally blind. Management for prevention of amblyopia was performed in treatable patients, although it still remains a life-long disability.

Opacity location plays an important role in the future of vision, although it is well-known that visual acuity will eventually be influenced by many factors. These factors include not only the location and density of the corneal opacity but also laterality, other ocular malformations, and systemic diseases, including intellectual growth. When we predict future vision of the patient, we have to take these factors into consideration.

Posterior segment abnormalities were identified by funduscope in 12 of 82 eyes (14.6%). Among patients who underwent B-mode echography, 125 eyes were without major disorders (90.6%). Thus, in our results, approximately 10% of ASD was combined with posterior segment abnormalities. The combination of posterior segment abnormalities seems to be not very common. Ocular findings were diverse, but they all were derived because of the arrest of some stage or stages of embryology. As reported previously by Trauboulsi and Maumenee,[4] anterior and posterior segment abnormalities exist as a complex malformative syndrome affecting the globe as a whole, rather than independently.

Systemic abnormalities were seen in 25.2% of our patients (Table 6), and this percentage is similar to that of the report from Rezende et al[1] (21.3%). Because nonocular neural crest cells form cartilage, bone, connective tissue, teeth components (except enamel), pigment cells, and peripheral nervous system of the face,[10] the majority of the systemic abnormalities also have their origin in the primary neural crest cell,[7] which is sometimes called systemic neurocristopathy.[24] Traboulsi and Maumenee[4] also suggest that midline body structures seem to be selectively involved in some patients with Peters anomaly, resulting from the contiguous gene syndrome or a defective homeotic gene controlling the development of the eye and body structure. Our results seem to support their theory.

TABLE 4. Posterior Segment Abnormalities Diagnosed by Funduscopy or B-mode Echography

Examination	Normal (%)	Abnormal (%)
Funduscopy (n = 82)	70 (85.4)	12 (14.6)
B-mode echography (n = 138)	125 (90.6)	13 (9.4)

n, number of eyes.

TABLE 6. Systemic Abnormalities Among Patients With ASD

Systemic Abnormalities	Cases (n = 139)	%
Multiple deformation	16	11.5
Cardiovascular disease	5	3.6
Neurologic disease	5	3.6
Craniofacial disease	3	2.2
Thyroid disease	2	1.4
Urinary disease	2	1.4
Otologic disease	2	1.4
No major complications	104	74.8

n, number of cases.

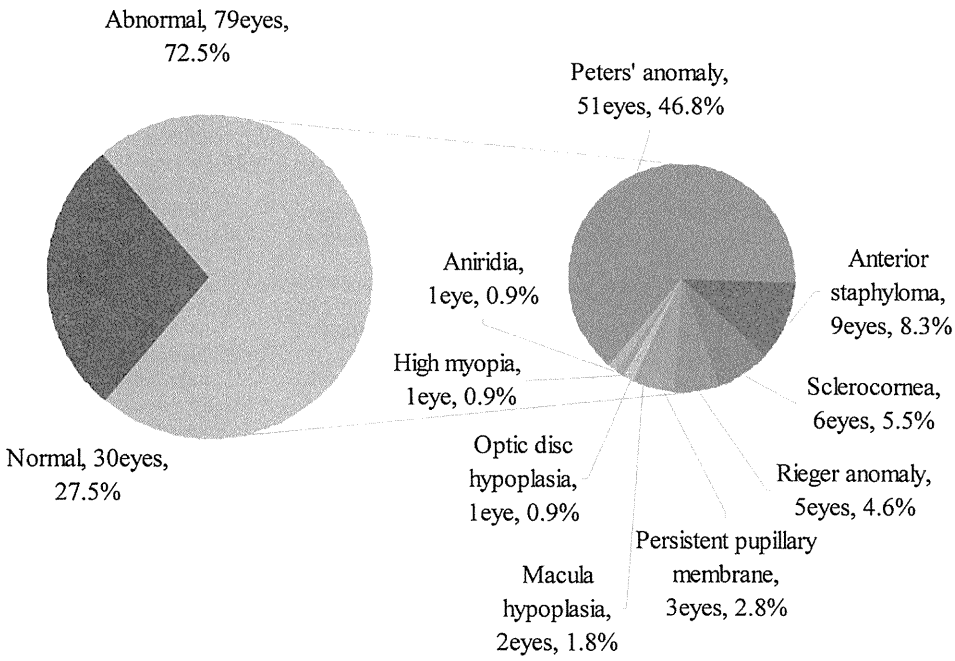

FIGURE 3. Diagnosis of the fellow eye in Peters anomaly (n = 109 eyes); 93.7% had bilateral ASD.

Family history was present in 3.6% of our patients. Rezende et al[1] reported 2 out of 47 patients to have a family history; hence, this percentage may be appropriate. In our study, most of the patients showed Peters anomaly. Peters anomaly is known to be sporadic, but sometimes it is inherited. Because Peters anomaly appeared in the majority in our study, this percentage may represent the frequency of inheritance of Peters anomaly.

As shown previously in our study, 72.5% of patients with Peters anomaly had bilateral ocular abnormalities. The majority (93.7%) had ASD, and two-thirds had Peters anomaly.

Peters anomaly was first reported by Von Hippel[25] in 1897, although the cause was unclear at that time. In 1906, Peters[26] defined it as a dysplasia of the anterior chamber, an incomplete separation between the lens capsule or iris tissue and the Descemet membrane.[20] The essential feature of Peters anomaly is a congenital central corneal opacity with defects in the posterior stroma, Descemet membrane, and endothelium.[6,13] It shows a wide range of morphological characteristics and severity. Some cases were complicated and difficult to diagnose under slit-lamp examination because the anterior chamber was invisible because of the severe corneal opacity.

High-frequency UBM[27–35] and AS-OCT[36] assistance were effective in these cases. The UBM method was reported in 1989 by Pavlin et al,[33] and the possibility of rendering images of the invisible anterior segment apparent made this apparatus come into wide use. Recently, another apparatus has been developed, and clinical data have been reported. Comparative studies evaluating AS-OCT show that it produces both more accurate and consistent images of the anterior segment compared with UBM.[36] However, limitation by the sclera and poor visualization of the ciliary body still remain a challenge to diagnosis by imaging.

ASD shows diverse clinical features, various severities of CCO, and visual outcomes. Clinical diagnosis of each eye may differ in bilateral cases. Further understanding of the disease as an abnormality during embryogenesis and neural crest cell differentiations may be required. Accurate diagnosis with UBM and AS-OCT assistance surely will be a step forward for the management of ASD-associated CCO in the future.

REFERENCES

1. Rezende RA, Uchoa UB, Uchoa R, et al. Congenital corneal opacities in a cornea referral practice. *Cornea*. 2004;23:565–570.
2. Haddad AM, Greenfield DS, Stegman Z, et al. Peter's anomaly: diagnosis by ultrasound biomicroscopy. *Ophthalmic Surg Lasers*. 1997;28:311–312.
3. Cotran PR, Bajart AM. Congenital corneal opacities. *Int Ophthalmol Clin*. 1992;32:93–105.
4. Traboulsi EI, Maumenee IH. Peters' anomaly and associated congenital malformations. *Arch Ophthalmol*. 1992;110:1739–1742.
5. Bermejo E, Martinez-Frias ML. Congenital eye malformations: clinical-epidemiological analysis of 1,124,654 consecutive births in Spain. *Am J Med Genet*. 1998;75:497–504.
6. Harissi-Dagher M, Colby K. Anterior segment dysgenesis: Peters anomaly and sclerocornea. *Int Ophthalmol Clin*. 2008;48:35–42.
7. Idrees F, Vaideanu D, Fraser SG, et al. A review of anterior segment dysgeneses. *Surv Ophthalmol*. 2006;51:213–231.
8. Churchill A, Booth A. Genetics of aniridia and anterior segment dysgenesis. *Br J Ophthalmol*. 1996;80:669–673.
9. Wilson ME. Congenital iris ectropion and a new classification for anterior segment dysgenesis. *J Pediatr Ophthalmol Strabismus*. 1990;27:48–55.
10. Beauchamp GR, Knepper PA. Role of the neural crest in anterior segment development and disease. *J Pediatr Ophthalmol Strabismus*. 1984;21:209–214.
11. Bahn CF, Falls HF, Varley GA, et al. Classification of corneal endothelial disorders based on neural crest origin. *Ophthalmology*. 1984;91:558–563.
12. Waring GO III, Rodrigues MM, Laibson PR. Anterior chamber cleavage syndrome. A stepladder classification. *Surv Ophthalmol*. 1975;20:3–27.
13. Kenyon KR. Mesenchymal dysgenesis in Peter's anomaly, sclerocornea and congenital endothelial dystrophy. *Exp Eye Res*. 1975;21:125–142.
14. Alkemade PP. Developmental disorders of the anterior ocular segment and xerosis conjunctivae. *Ophthalmologica*. 1968;155:317–329.
15. Sowden JC. Molecular and developmental mechanisms of anterior segment dysgenesis. *Eye (Lond)*. 2007;21:1310–1318.
16. Alward WLM. Axenfeld-Rieger syndrome and Peters anomaly. In: Krachmer JH, Mannis MJ, Holland EJ, eds. *Cornea*. 2nd ed. St. Louis, MO: Mosby; 2005:745–748.

17. Nischal KK. Congenital corneal opacities—a surgical approach to nomenclature and classification. *Eye (Lond)*. 2007;21:1326–1337.
18. Ciralsky J, Colby K. Congenital corneal opacities: a review with a focus on genetics. *Semin Ophthalmol*. 2007;22:241–246.
19. Zaidman GW, Juechter K. Peters' anomaly associated with protruding corneal pseudo staphyloma. *Cornea*. 1998;17:163–168.
20. Mayer UM. Peters' anomaly and combination with other malformations (series of 16 patients). *Ophthalmic Paediatr Genet*. 1992;13:131–135.
21. Leff SR, Shields JA, Augsburger JJ, et al. Congenital corneal staphyloma: clinical, radiological, and pathological correlation. *Br J Ophthalmol*. 1986;70:427–430.
22. Clementi M, Bianchi F, Calabro A, et al. Eye malformations: an epidemiological study in a million births in Italy. Presented at: 25th Annual Meeting of the European Society of Human Genetics Book of Abstracts, Barcelona, Spain; May 6–9, 1993; 45.
23. EUROCAT Working Group. *Surveillance of Congenital Anomalies 1980-1992. EUROCAT Report 6*. Brussels, Belgium: Institute of Hygiene and Epidemiology; 1995:46–55.
24. Steinsapir KD, Lehman E, Ernest JT, et al. Systemic neurocristopathy associated with Rieger's syndrome. *Am J Ophthalmol*. 1990;110: 437–438.
25. Von Hippel E. Uber hydrophthalmus congenitus nebst bemerkungen uber die verfarbung der cornea durch blufarbstoff; Pathologisch-anatomische untersucuchungen. *Albrecht von Graefe's Arch Ophthalmol*. 1897;44:539–564.
26. Peters A. Uber angeborene Defektbildung des Descemet'schen Membran. *Klin Monatsbl Augenheilkd*. 1906;44:27–40.
27. Nischal KK, Naor J, Jay V, et al. Clinicopathological correlation of congenital corneal opacification using ultrasound biomicroscopy. *Br J Ophthalmol*. 2002;86:62–69.
28. Kiryu J, Park M, Kobayashi H, et al. Ultrasound biomicroscopy of the anterior segment of the eyes of infants. *J Pediatr Ophthalmol Strabismus*. 1998;35:320–322.
29. Avitabile T, Russo V, Ghirlanda R, et al. Corneal oedemas: diagnosis and surgical planning with ultrasound biomicroscopy. *Ophthalmologica*. 1998;212(Suppl 1):13–16.
30. Kobayashi H, Kiryu J, Kobayashi K, et al. Ultrasound biomicroscopic measurement of anterior chamber angle in premature infants. *Br J Ophthalmol*. 1997;81:460–464.
31. Azuara-Blanco A, Spaeth GL, Araujo SV, et al. Ultrasound biomicroscopy in infantile glaucoma. *Ophthalmology*. 1997;104:1116–1119.
32. Pavlin CJ, Harasiewicz K, Sherar MD, et al. Clinical use of ultrasound biomicroscopy. *Ophthalmology*. 1991;98:287–295.
33. Pavlin CJ, Sherar MD, Foster FS. Subsurface ultrasound microscopic imaging of the intact eye. *Ophthalmology*. 1990;97:244–250.
34. Park M, Kiryu J, Kurimoto Y, et al. [Ultrasound biomicroscopic observation of the anterior eye segment in a sclerocornea and a microcornea]. *Nippon Ganka Gakkai Zasshi*. 1997;101:69–73.
35. Kim T, Cohen EJ, Schnall BM, et al. Ultrasound biomicroscopy and histopathology of sclerocornea. *Cornea*. 1998;17:443–445.
36. Ramos JL, Li Y, Huang D. Clinical and research applications of anterior segment optical coherence tomography—a review. *Clin Experiment Ophthalmol*. 2009;37:81–89.

Clinical Features of Congenital Retinal Folds

SACHIKO NISHINA, YUMI SUZUKI, TADASHI YOKOI, YURI KOBAYASHI, EIICHIRO NODA, AND NORIYUKI AZUMA

• PURPOSE: To investigate the clinical features and prognosis of congenital retinal folds without systemic associations.

• DESIGN: Retrospective observational case series.

• METHODS: The characteristics, clinical course, ocular complications, and best-corrected visual acuity (BCVA) of eyes with congenital retinal folds were studied during the follow-up periods. The affected and fellow eyes were examined by slit-lamp biomicroscopy, binocular indirect ophthalmoscopy, and fundus fluorescein angiography. The parents and siblings of each patient also underwent ophthalmoscopic examinations. The BCVA was measured using a Landolt ring VA chart.

• RESULTS: One hundred forty-seven eyes of 121 patients with congenital retinal folds were examined. Fifty-five patients (45.5%) were female. The fold was unilateral in 95 patients (78.5%), and 69 of those patients (72.6%) had retinal abnormalities in the fellow eye. The meridional distribution of folds was temporal in 136 eyes (92.5%). The family history was positive in 32 patients (26.4%). Secondary fundus complications, including fibrovascular proliferation and tractional, rhegmatogenous, and exudative retinal detachments, developed in 44 eyes (29.9%). The BCVAs could be measured in 119 eyes and ranged from 20/100 to 20/20 in 5 eyes (4.2%), 2/100 to 20/200 in 45 eyes (37.8%), and 2/200 or worse in 69 eyes (58.0%). The follow-up periods ranged from 4 to 243 months (mean, 79.7 ± 58.9 months).

• CONCLUSIONS: These clinical features suggested that most congenital retinal folds may result from insufficient retinal vascular development, as in familial exudative vitreoretinopathy, rather than persistent fetal vasculature. Adequate management of active retinopathy and late-onset complications, especially retinal detachment, is required. (Am J Ophthalmol 2012;153:81–87.

A CONGENITAL RETINAL FOLD (ABLATIO FALCIFORmis congenital), extending radially from the optic disc toward the peripheral fundus, was first described in 1935 as a rare congenital anomaly.[1,2] The pathogenesis was investigated histologically, and the anomaly was hypothesized to be attributable to persistent hyaloid vessels leading to a pulled dysplastic retina. In 1955, Reese reported the clinical and pathologic features of persistent hyperplastic primary vitreous (PHPV).[3] In 1965, Michaelson[4] introduced the term "posterior PHPV,"[4] and in 1970 Pruett and Schepens[5] described a new clinical entity called "posterior hyperplastic primary vitreous," the posterior form of PHPV, characterized by vitreous membranes extending from the disc toward the peripheral fundus. Those investigators used the term posterior PHPV as a synonym for falciform retinal folds and the term anterior PHPV as a synonym for the PHPV described by Reese.[3] Thus, congenital retinal folds often were diagnosed as posterior PHPV afterward. The term PHPV now has evolved to persistent fetal vasculature (PFV), which usually occurs as a nonheritable set of vascular malformations affecting 1 eye of an otherwise normal infant.[6] However, based on the fundus drawings of Pruett and Schepens,[5] vitreous membranes and retinal folds were not clearly distinguished. Those authors reported that the vitreous band and retinal folds extended toward the fundus periphery in various meridians but were most commonly nasal.[5] They also described the pleomorphism of posterior PHPV and complications such as microcornea, retinal detachment, vitreous hemorrhage, cataract, and glaucoma.[7] In most cases, posterior PHPV is unilateral and rarely familial.

In 1969, familial (dominant) exudative vitreoretinopathy (FEVR), a developmental disorder of the retinal vasculature, was described and suggested to be the possible origin of congenital retinal folds.[8–10] Recently, congenital retinal folds were thought to occur even after birth and were caused by various infantile diseases such as FEVR, retinopathy of prematurity (ROP), Norrie disease, incontinentia pigmenti, and congenital toxoplasmosis. However, clinically distinguishing retinal folds without systemic associations is often difficult, and their pathogenesis remains controversial.

We conducted the current study to clarify the clinical features of congenital retinal folds without systemic associations.

METHODS

ONE HUNDRED FORTY-SEVEN EYES OF 121 PATIENTS WITH unilateral or bilateral congenital retinal folds, diagnosed at the National Center for Child Health and Development,

Accepted for publication Jun 6, 2011.

From the Division of Ophthalmology, National Center for Child Health and Development, Tokyo, Japan.

Inquiries to Noriyuki Azuma, Division of Ophthalmology, National Center for Child Health and Development, 2-10-1 Ohkura, Setagaya-ku, Tokyo, 157-8535, Japan; e-mail: azuma-n@ncchd.go.jp

0002-9394/$36.00
doi:10.1016/j.ajo.2011.06.002

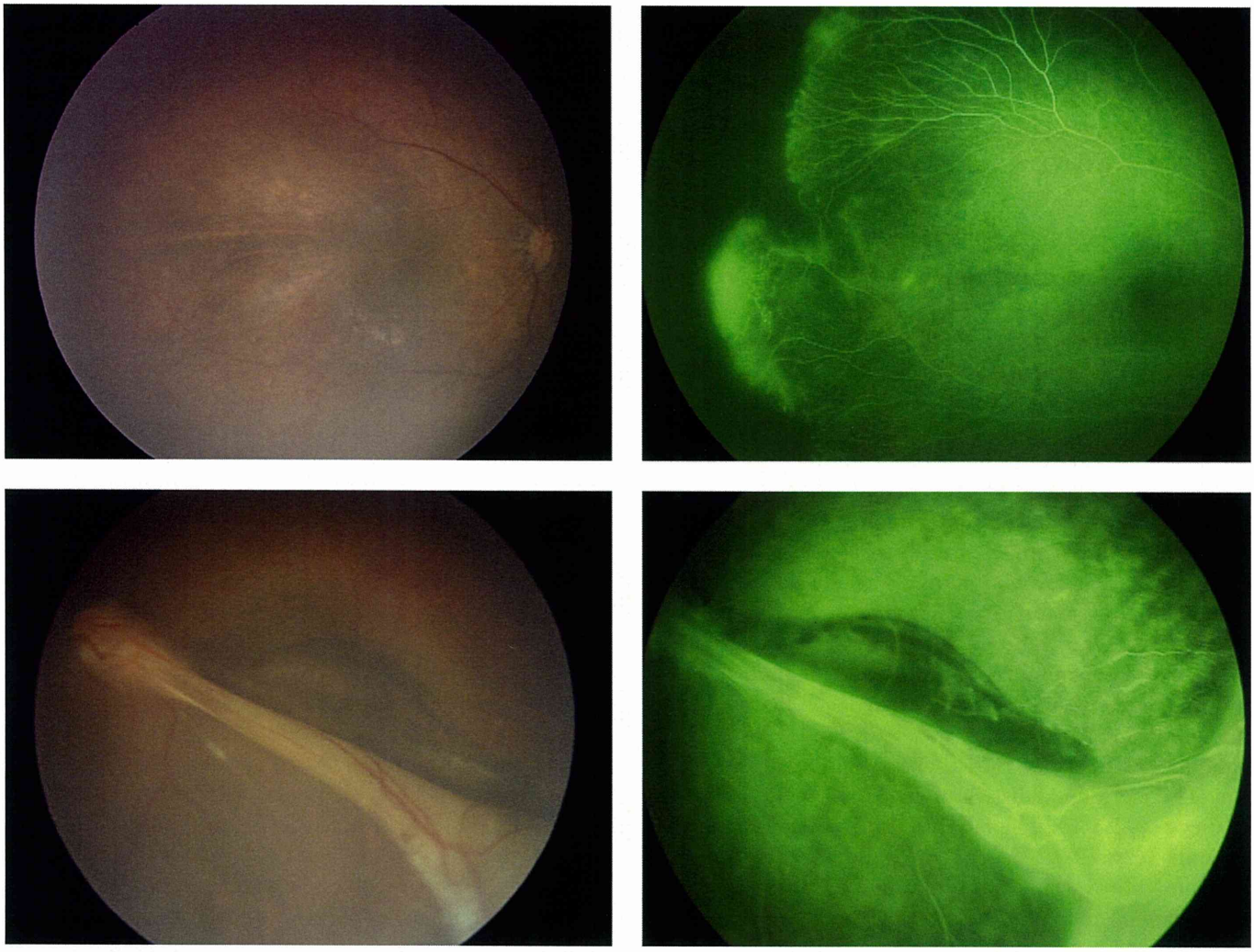

FIGURE 1. Unilateral congenital fold with retinal vascular abnormalities in the fellow eye. Fundus photographs and fluorescein angiography (FA) of a unilateral retinal fold in the left eye (Bottom left and right) and the fellow right eye (Top left and right) in a 4-month-old boy. (Top left) Retinal vascular abnormalities in the peripheral fundus are seen in the fellow right eye. (Top right) FA shows a peripheral avascular zone, supernumerous vascular branchings, arteriovenous shunt formation, a V-shaped area of degeneration, and neovascularization with dye leakage in the fellow right eye. Laser photocoagulation was applied to the peripheral avascular retina. (Bottom left) The retinal vessels within the fold are bundled and pulled toward the peripheral fibrous tissue and decreased in number in the stretched retina. (Bottom right) FA shows hyperfluorescence from folds in which the vessels are bundled and dye leakage from the fibrovascular tissue. Scleral buckling with laser photocoagulation was applied.

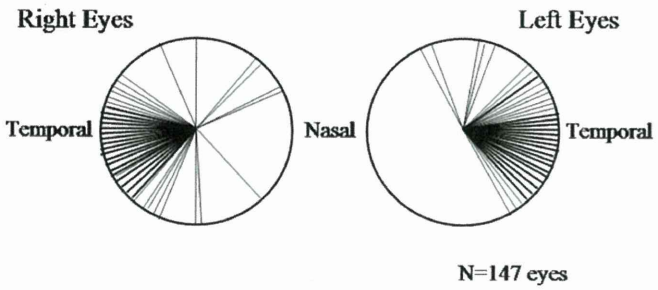

FIGURE 2. Meridional distribution of congenital retinal folds. The meridional distribution of the folds was temporal, superotemporal, or inferotemporal in 92.5% (136/147) eyes.

Tokyo, Japan, between June 1986 and February 2009, and examined between March 2002 and April 2009, were studied retrospectively. Patients with a history of premature birth, oxygen therapy, systemic associations, or positive laboratory examinations for infectious diseases were excluded. Eyes with anterior segment dysgenesis also were excluded.

The characteristics of retinal folds in affected eyes and findings in fellow eyes were examined by slit-lamp biomicroscopy and binocular indirect ophthalmoscopy. Thirty-six patients (29.8%) underwent fundus fluorescein angiography (FA) under general anesthesia. In patients with a unilateral retinal fold, the fundus periphery of the fellow eye also was examined and the retinal vascular development was evaluated. The criteria used to diagnose

TABLE. Features of Secondary Ocular Complications in the Fundus in Eyes With Congenital Retinal Folds (N = 44 Eyes)

	Tractional Retinal Detachment N = 19 Eyes	Rhegmatogenous Retinal Detachment N = 12 Eyes	Fibrovascular Proliferation N = 11 Eyes	Exudative Retinal Detachment N = 2 Eyes
Age at onset (months)	1–88 (mean, 25.8 ± 27.2)	33–195 (mean, 87.0 ± 56.5)	2–121 (mean, 19.4 ± 35.8)	31, 167
Origin of complications	Excessive fibrovascular proliferation, 15 (79%) Regrowth of fibrovascular tissue, 4 (21%)	Ocular trauma, 5 (42%) Unknown, 7 (58%)	NV, 10 (91%) Recurrence of NV, 1 (9%)	Unknown 2 (100%)
Treatment	V + L, 6 (32%) B + PC, 4 (21%) None, 9 (47%)	V + L, 5 (42%) V + L + B, 4 (33%) B, 2 (17%) None, 1 (8%)	V + L, 5 (46%) PC, 4 (36%) B + PC, 1 (9%) None, 1 (9%)	None, 2 (100%)[a]
Surgical outcomes	Retinal reattachment, 7/10 (70%)	Retinal reattachment, 3/11 (27%)	NV stabilization, 8/10 (80%)	

B = scleral buckling; B + PC = scleral buckling with laser photocoagulation; NV = neovascularization; PC = laser photocoagulation; V + L = vitrectomy with lensectomy; V + L + B = vitrectomy with lensectomy and scleral buckling.
[a]Untreated retinas reattached spontaneously.

retinal vascular abnormalities were the presence of a peripheral avascular zone, vitreoretinal adhesions, arteriovenous shunt formation, supernumerous vascular branchings, a V-shaped area of retinal degeneration, neovascularization, and cystoid degeneration.[11–13] Ophthalmoscopic examinations of the parents and siblings of each patient were performed when possible. A family history was judged to be present if retinal vascular abnormalities were found in any family members. The clinical course and the secondary ocular complications were investigated during the follow-up periods. The best-corrected visual acuities (BCVAs) were measured with a standard Japanese VA chart using Landolt rings at 5 meters and converted to Snellen VA. The follow-up periods ranged from 4 to 243 months (mean, 79.7 ± 58.9 months).

RESULTS

• CHARACTERISTICS OF EYES AND PATIENTS: Sixty-six of the 121 patients (54.5%) were male and 55 (45.5%) were female. The ages of the patients at the first examination at our hospital ranged from 4 weeks to 9 years 1 month (mean, 17.9 ± 21.6 months). However, the families or pediatricians had observed the clinical manifestations, that is, poor fixation behavior, nystagmus, or strabismus, by 12 months of age in 105 patients (86.8%), and 91 patients (75.2%) had been examined by other ophthalmologists within the first year. A unilateral retinal fold in 16 patients (13.2%) identified after 13 months of age was confirmed not to have any acquired pathogenesis and diagnosed as a congenital retinal fold.

The retinal vessels within the fold were bundled and pulled toward the peripheral fibrous tissue and decreased in number in the stretched retina in 144 of 147 eyes (98.0%) (Figure 1, Bottom left). A peripheral avascular zone was seen more than 3 disc diameters' width in all eyes. Other ophthalmoscopic findings in affected eyes were intravitreal neovascularization in 13 eyes (8.8%), retinal hemorrhages in 8 eyes (5.4%), disc anomalies in 4 eyes (2.7%), retinal exudates in 3 eyes (2.0%), and coloboma and medullated nerve fiber in 1 eye (0.7%) each. Fundus FA, performed on 46 eyes of 36 patients, showed hyperfluorescence from bundling of the retinal vessels in the folds and fibrovascular tissue at the periphery of the folds in all eyes (100%). Dye leakage from an arteriovenous shunt and intravitreal neovascularization within the fibrovascular tissue was detected in 13 eyes (28.3%) (Figure 1, Bottom right).

• MOST CASES OF CONGENITAL RETINAL FOLD WERE UNILATERAL AND ORIGINATED IN THE TEMPORAL QUADRANTS: The fold was unilateral in 95 of 121 patients (78.5%) and bilateral in 26 patients (21.5%). The meridional distribution of the folds was temporal, superotemporal, or inferotemporal in 136 of 147 eyes (92.5%) (Figure 2). All folds in the other 11 eyes were unilateral, extending nasally, superonasally, inferonasally, superiorly, or inferiorly.

• MOST CASES OF UNILATERAL RETINAL FOLD HAD IDENTIFIABLE ABNORMALITIES IN THE FELLOW EYE: Only 26 cases (27.4%) of the 95 unilateral retinal folds identified demonstrated no pathology in the fellow eye. The remaining 72.6% had identifiable abnormalities as

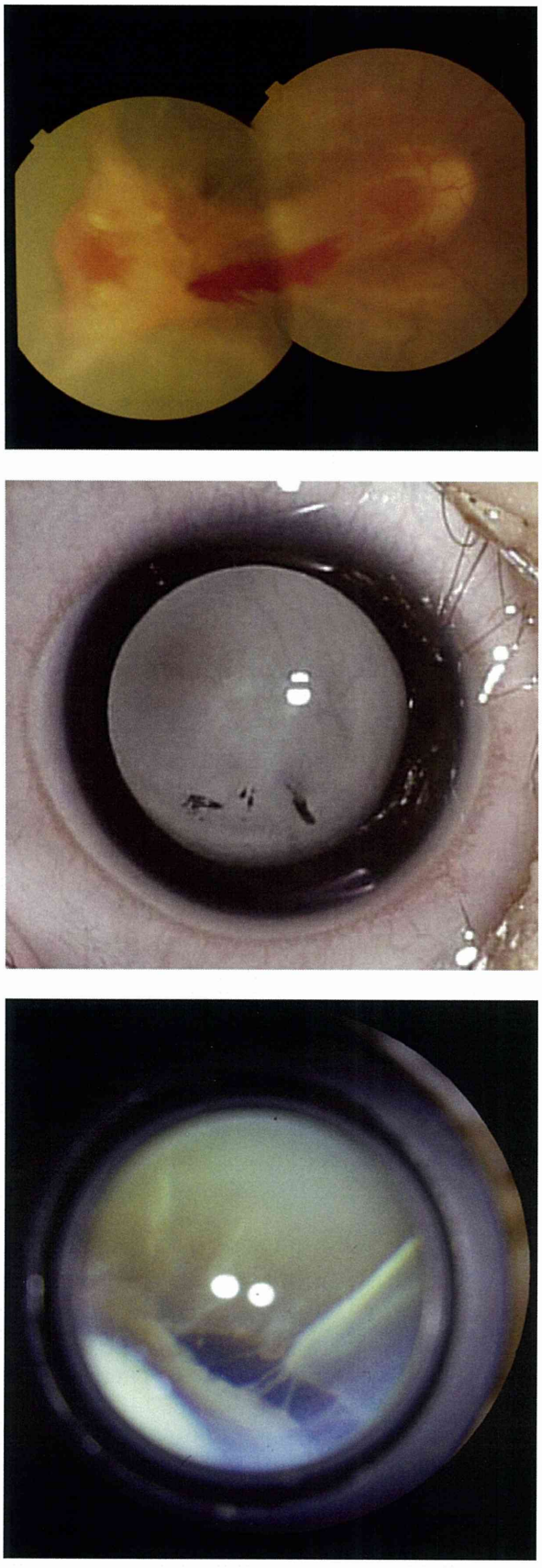

FIGURE 3. Secondary complications of congenital retinal folds. Photographs of secondary complications in the fundus of a 4-month-old girl (Top and Middle) and a 37-month-old boy (Bottom). (Top) Prominent fibrovascular proliferation progresses with the retinal hemorrhage in the right eye. Laser photocoagulation was applied to the peripheral avascular retina. (Middle) Two months later, a tractional retinal detachment has progressed rapidly. Vitrectomy with lensectomy was performed. (Bottom) Multiple retinal breaks in the periphery at the edge of the retinal fold have induced a rhegmatogenous retinal detachment in the left eye. Vitrectomy with lensectomy and scleral buckling were performed.

follows. Retinal vascular abnormalities in the peripheral fundus were identified in 33 of 95 cases (34.7%): an avascular zone in all eyes (100%), supernumerous vascular branchings in 15 eyes (45.5%), cystoid degeneration in 12 eyes (36.4%), a V-shaped area of retinal degeneration in 9 eyes (27.3%), vitreoretinal adhesions and fibrous membrane in 7 eyes (21.2%) each, arteriovenous shunt formation in 5 eyes (15.2%), and neovascularization in 4 eyes (12.1%) (Figure 1, Top left and right). A total retinal detachment and leukokoria, a dragged retina, and coloboma were found in 18 (18.9%), 17 (17.9%), and 1 (1.1%) of 95 cases, respectively.

The "true" unilateral congenital fold was seen in 26 patients out of all 121 patients (21.5%). Among these 26 patients, the meridional distribution of the folds was temporal in 17 eyes (65.4%) and nasally, superiorly, or inferiorly in 9 eyes (34.6%).

Fundus FA was performed on 24 fellow eyes in patients with a unilateral retinal fold and clearly showed various retinal vascular abnormalities in 18 eyes (75.0%). Hyperfluorescence of the vascular abnormalities in the periphery was seen in 8 of the 24 eyes (33.3%), in which dye leakage from the neovascularization was detected in 4 eyes (4/24; 16.7%) (Figure 1, Top right).

Among the 50 fellow eyes with retinal vascular abnormalities in the periphery or dragged retina, laser photocoagulation was applied to the peripheral avascular retina in 7 eyes (14.0%) and the neovascularization stabilized in all eyes (100%). Scleral buckling was performed in 3 fellow eyes (6.0%) for a late-onset tractional or rhegmatogenous retinal detachment, and retinal reattachment was achieved in all eyes (100%).

• MOST CASES OF CONGENITAL RETINAL FOLD SUGGEST FAMILIAL INHERITANCE: Family members were examined in 50 cases (41.3%), and a positive family history was identified in 32 cases (64.0%), with ophthalmoscopic findings of retinal vascular abnormalities in the periphery (81.2%), retinal folds (9.4%), dragged retina (6.3%), and leukokoria (3.1%). A negative family history was suspected by ocular examination of the parents in 18 cases (36.0%). In all cases with a positive family history, the trait originated in 1 of the family lines. In positive cases, the fold was bilateral in 12 cases (37.5%) and unilateral with abnormal retinal vascular changes in the fellow eye in the other 20 cases (62.5%). In negative cases,

the fold was bilateral in 5 cases (27.8%), unilateral with abnormal retinal vascular change in the fellow eye in 9 cases (50.0%), and unilateral with normal fellow eye in 4 cases (22.2%).

• SECONDARY COMPLICATIONS OF CONGENITAL RETINAL FOLD ARE COMMON AND VISUALLY DEVASTATING: During the follow-up periods, secondary ocular complications developed in the fundus in 44 of 147 eyes (29.9%) with congenital retinal folds; progression of a tractional retinal detachment in 19 eyes (12.9%), rhegmatogenous retinal detachment in 12 eyes (8.2%), fibrovascular proliferation from the neovascularization in 11 eyes (7.5%), and exudative retinal detachment in 2 eyes (1.4%). The secondary complications in the fundus of 44 eyes are summarized in the Table.

Among the 26 patients with "true" unilateral congenital fold, secondary ocular complications also developed in the fundus in 6 eyes (23.1%); progression of a tractional retinal detachment in 2 eyes (7.7%), rhegmatogenous retinal detachment in 1 eye (3.8%), fibrovascular proliferation from the neovascularization in 2 eyes (7.7%), and exudative retinal detachment in 2 eyes (3.8%).

• TRACTIONAL RETINAL DETACHMENTS: Progression of tractional retinal detachment occurred in patients ranging in age from 1 to 88 months (mean, 25.8 ± 27.2 months). Among the 19 eyes the tractional retinal detachment originated from excessive fibrovascular proliferation and contraction in 15 eyes (79%) (Figure 3, Top and Middle) and regrowth of fibrovascular tissue in 4 eyes (21%). Ten eyes (53%) were treated: vitrectomy with lensectomy was performed in 6 eyes (32%) and scleral buckling with laser photocoagulation in 4 eyes (21%). Retinal reattachment was achieved in 7 of 10 treated eyes (70%).

• RHEGMATOGENOUS RETINAL DETACHMENTS: A rhegmatogenous retinal detachment developed in patients ranging in age from 33 to 195 months (mean, 87.0 ± 56.5 months). Among the 12 eyes, ocular trauma including the digito-ocular sign was involved in 5 eyes (42%). Multiple or expanded retinal breaks were seen in the periphery within the stretched and fragile retina at the edge of the retinal folds in 8 eyes (67%) (Figure 3, Bottom), dialysis developed in 1 eye (8.3%), and no breaks were seen in 3 eyes. Nine eyes (75%) with a rhegmatogenous retinal detachment had a total retinal detachment with proliferative vitreoretinopathy (PVR). Treatment was performed in 11 eyes (92%): vitrectomy with lensectomy in 5 eyes (42%), vitrectomy with lensectomy and scleral buckling in 4 eyes (33%), and scleral buckling in 2 eyes (17%); however, retinal reattachment occurred in 3 of 11 treated eyes (27%).

• FIBROVASCULAR PROLIFERATION: Fibrovascular proliferation progressed in patients ranging in age from 2 to 121 months (mean, 19.4 ± 35.8 months), within the first year in 9 of 11 eyes (82%). Growth of neovascularization was identified in 11 eyes (100%). Treatment was performed in 10 eyes (91%): vitrectomy with lensectomy in 5 eyes (46%), laser photocoagulation applied to the peripheral avascular retina in 4 eyes (36%), and scleral buckling with laser photocoagulation in 1 eye (9%); treatment stabilized the neovascularization and prevented a retinal detachment in 8 of 10 treated eyes (80%).

• ANTERIOR SEGMENT COMPLICATIONS: Secondary complications in the anterior segments developed in 16 of 147 eyes (10.9%) with congenital retinal folds; glaucoma in 9 eyes (6.1%), cataract in 8 eyes (5.4%), and band keratopathy and keratoconus in 1 eye (0.7%) each. Two glaucoma eyes developed cataracts and 1 cataract eye developed glaucoma after cataract surgery. Glaucoma developed in patients ranging in age from 2 to 137 months (mean, 60.1 ± 46.8 months). The main cause was fibrovascular proliferation and contraction that resulted in anterior lens displacement and angle-closure glaucoma. Neovascular glaucoma was identified in 1 eye. Treatment was performed in 6 eyes (67%): medical treatment in 4 eyes and lensectomy and peripheral iridectomy in 1 eye each. Cataract developed in patients ranging in age from 11 to 113 months (mean, 59.1 ± 40.2 months). Lensectomy was performed in 4 eyes (50%).

Among the 26 patients with "true" unilateral congenital fold, secondary complications in the anterior segments developed in 4 eyes (15.4%): glaucoma in 1 eye (3.8%) and cataract in 3 eyes (11.5%).

• VISUAL OUTCOMES WERE GENERALLY POOR: The VA could be measured in 119 eyes. Of these, the final BCVA ranged from 20/100 to 20/20 in 5 eyes (4.2%) with macular formation, 2/100 to 20/200 in 45 eyes (37.8%), 2/200 to light perception in 46 eyes (38.7%), and no light perception in 23 eyes (19.3%). Among the total of 147 eyes, an ocular prosthesis was used in 8 eyes (5.4%) with phthisis bulbi or microphthalmos to facilitate orbital growth.

DISCUSSION

IN THE CURRENT SERIES, THE RETINAL VESSELS WITHIN THE folds were bundled and pulled toward the temporal periphery in most cases. The retinal vessels may appear not to enter the fold but to have developed before the retina became folded. The folds mostly were composed of stretched retina rather than vitreous membranes, described by Michaelson[4] and by Pruett and Schepens,[5] extending from the disc toward the peripheral fundus. Pruett and Schepens reported that the meridional distribution of

vitreous bands and retinal folds was commonly on the nasal side,[5] but in the current study, the folds extended temporally in 92.5% (136/147) eyes, although in the "true" unilateral congenital fold group of 26 patients (26 eyes), the folds extended nasally, superiorly, or inferiorly in higher rate of 34.6% (9/26) eyes compared to 7.5% (11/147) eyes.

The affected eye also had a peripheral avascular zone and retinal vascular abnormalities including neovascularization, hemorrhage, and exudates that indicated active retinopathy. The retinal folds were unilateral in 78.5% of eyes; however, 71.5% of patients with a unilateral fold had abnormal retinal vascular changes, a dragged retina, or total retinal detachment and leukokoria in the fellow eye. Insufficient retinal vascular development and abnormal vascular changes were seen frequently in the temporal periphery of the fellow eyes (34.7%). Since the growth of retinal vessels is more likely to be delayed temporally than nasally, these features seemed to indicate that most retinal folds in the current series may have resulted from bilateral incomplete and abnormal vascular retinal development, similar to that of ROP. Most congenital retinal folds may be caused by insufficient retinal vascular development, as in FEVR, rather than by PFV. It is interesting that features in each eye of the same patient are often quite different in this series. It is distinctly unusual in ROP for patients to develop severe retinopathy in 1 eye but not develop a similar degree of pathology in the other eye. Insufficiency of vascular development of this series may originate from gene mutations that related to morphogenesis of the retinal vessels. The molecular mechanism needs further elucidation.

The family history was positive in 64.0% of cases in which family members were examined. All positive cases had bilateral manifestations of incomplete and abnormal vascular development that confirmed the diagnosis of FEVR. Most positive cases were transmitted by autosomal dominant inheritance, while none was transmitted by autosomal recessive or X-linked recessive inheritance. Sporadic cases may exist within 77.8% of negative cases with bilateral manifestations. Gene studies to detect mutations in *FZD4*, *LRP5*, and *NDP* are under way to clarify the genetic characteristics of Japanese patients.

Regarding secondary fundus complications, a high rate of fibrovascular proliferation and rapid progression of tractional retinal detachments indicate the characteristics of active FEVR. Van Nouhuys[9] and Nishimura and associates[10] reported similar features of retinal folds. Various retinal involvements in FEVR have been studied and reported since 1982 in Japan.[10–12] There may be differences among races, but FEVR is supposed to be a rather common origin of congenital retinal folds without systemic associations.

The "true" unilateral congenital fold, the small group of patients that most closely resemble "congenital retinal folds" as previously described, seems to have different pathology. PFV may play a role in the pathogenesis of congenital retinal folds in unilateral cases, especially those associated with coloboma in the affected or fellow eye,[14] in which a tent-shaped retinal detachment (fold) extends inferiorly along with the fetal fissure. In those cases, the tractional fetal tissue pulled on the retina and caused a tent-like configuration.[7] The term anterior-peripheral PFV and not posterior PHPV should be used for the origin of congenital retinal folds pulled by the fetal fibrous tissue in the periphery. However, it is rare that PFV results in peripheral fibrous proliferation, because PFV usually proliferates along the hyaloid artery.

Few reports have been published on the long-term prognosis of retinal folds. Van Nouhuys reported that 3 different factors play an etiologic role in the pathogenesis of retinal detachments in eyes with FEVR: traction from vitreous membranes, atrophy of the peripheral retina, and subretinal exudation.[15] In that study, the most frequent late complication was a retinal detachment, which developed in 20% of 180 eyes with FEVR, and traction was the most important cause of the retinal detachment. Recently, surgery, including peripheral laser ablation and vitrectomy, has been advocated in FEVR including retinal folds. Previous reports of vitrectomy to treat FEVR mainly involved cases of tractional retinal detachment.[16,17]

In the current study, nearly 30% of affected eyes with congenital retinal folds developed secondary fundus complications including fibrovascular proliferation, tractional retinal detachment, rhegmatogenous retinal detachment, and exudative retinal detachment. Even in the group of patients with "true" unilateral congenital fold, secondary fundus complications developed in 23.1%. The complication rate with the "true" unilateral fold seems to be also high in fundus and rather higher in the anterior segments.

Fibrovascular proliferation developed from neovascularization of active retinopathy in 7.5% of eyes, mostly within the first year of life. Tractional retinal detachments developed from excessive fibrovascular proliferation and regrowth in 12.9% in infants and younger children under 4 years of age. However, it is noteworthy that fibrovascular proliferation and tractional retinal detachments may develop from regrowth in older children aged 7 to 10 years. Meanwhile, rhegmatogenous retinal detachments and exudative retinal detachments developed in 8.2% and 1.4%, respectively, in older children from 2 to 16 years old. Ocular trauma was highly involved in the development of rhegmatogenous retinal detachments. Retinal breaks mostly occurred in the periphery within the stretched retinal folds, resulting in intractable PVR. Laser photocoagulation, scleral buckling, and vitrectomy with lensectomy were performed in the affected eyes with useful vision; however, the success rates for eyes complicated with fibrovascular proliferation, a tractional retinal detachment, and a rhegmatogenous retinal detachment were 80%, 70%, and 27%, respectively.

These results indicated that very early diagnosis within the first months of life, frequent examinations at a young age, and early intervention with laser and vitreoretinal surgery are essential to prevent serious complications and preserve useful vision. Fundus FA is recommended in cases suspected to arise from neovascularization of active retinopathy. The current findings also confirmed the need for a thorough ophthalmoscopic examination of the fellow eye in patients with unilateral retinal folds and for examinations of siblings at an early age. Early detection of a retinal detachment was extremely hard in eyes with a unilateral fold or in worse eyes with bilateral folds. We also recommend that older children undergo follow-up every 3 months, avoid sports associated with a high risk of ocular trauma, and wear protective glasses. Secondary complications in the anterior segment also developed in nearly 11% with congenital retinal folds in the current series. Glaucoma and cataract developed in 6.1% and 5.4%, respectively, in patients around 5 years of age; however, those diseases may develop in infants to older children older than 9 years of age. Longer follow-up may increase the morbidity of the anterior and posterior complications. Thus, life-long observation is needed to preserve vision in eyes with a retinal fold.

The final BCVAs were 20/100 to 20/20 in 5 eyes (4.2%), 2/100 to 20/200 in 45 eyes (37.8%), and 2/200 or worse in 69 eyes (58.0%), because the temporal retina including the macula was folded in most eyes. In 5 eyes with VA of 20/100 or better, the folds were pulled nasally, superiorly, or inferiorly to the periphery and the normal macular morphology was preserved. It is suggested that even in eyes with congenital retinal folds, if the macular is rotated, appropriate treatment for amblyopia should be performed to facilitate development of good vision and binocular function.[18]

PUBLICATION OF THIS ARTICLE WAS SUPPORTED BY HEALTH AND LABOUR SCIENCES RESEARCH GRANTS OF RESEARCH ON intractable diseases from the Ministry of Health, Labour and Welfare, Tokyo, Japan. Funding sources had no role in the design or conduct of this study. Involved in design and conduct of the study (S.N., N.A.); collection, management, analysis, and interpretation of the data (S.N., Y.S., T.Y., Y.K., E.N., N.A.); and preparation, review, and approval of the manuscript (S.N., Y.S., T.Y., Y.K., E.N., N.A.). This study was approved by the institutional ethics committee of the National Center for Child Health and Development; the parents of the patients provided informed consent before the infants were enrolled.

REFERENCES

1. Mann I. Congenital retinal fold. Br J Ophthalmol 1935; 19(12):641–658.
2. Weve H. Ablatio falciformis congenita (retinal fold). Br J Ophthalmol 1938;22(8):456–470.
3. Reese AB. Persistent hyperplastic primary vitreous. Am J Ophthalmol 1955;40(3):317–331.
4. Michaelson IC. Intertissue vascular relationship in the fundus of the eye. Invest Ophthalmol 1965;4(6):1004–1015.
5. Pruett RC, Schepens CL. Posterior hyperplastic primary vitreous. Am J Ophthalmol 1970;69(4):535–543.
6. Goldberg MF. Persistent fetal vasculature (PFV): an integrated interpretation of signs and symptoms associated with persistent hyperplastic primary vitreous (PHPV). Am J Ophthalmol 1997;124(5):587–626.
7. Pruett RC. The pleomorphism and complications of posterior hyperplastic primary vitreous. Am J Ophthalmol 1975; 80(4):625–629.
8. Criswick VG, Schepens CL. Familial exudative vitreoretinopathy. Am J Ophthalmol 1969;68(4):578–594.
9. Van Nouhuys CE. Congenital retinal fold as a sign of dominant exudative vitreoretinopathy. Albrecht von Graefes Arch Klin Ophthalmol 1981;217(1):55–67.
10. Nishimura M, Yamana T, Sugino M, et al. Falciform retinal fold as sign of familial exudative vitreoretinopathy. Jpn J Ophthalmol 1983;27(1):40–53.
11. Miyakubo H, Inohara N, Hashimoto K. Retinal involvement in familial exudative vitreoretinopathy. Ophthalmologica 1982;185(3):125–135.
12. Miyakubo H, Hashimoto K, Miyakubo S. Retinal vascular pattern in familial exudative vitreoretinopathy. Ophthalmology 1984;91(12):1524–1530.
13. Pendergast SD, Trese MT. Familial exudative vitreoretinopathy. Result of surgical management. Ophthalmology 1998(6); 105:1015–1023.
14. Suzuki Y, Kawase E, Nishina S, Azuma N. Two patients with different features of congenital optic disc anomalies in the two eyes. Graefes Arch Clin Exp Ophthalmol 2006;244(2): 259–261.
15. Van Nouhuys CE. Juvenile retinal detachment as a complication of familial exudative vitreoretinopathy. Fortschr Ophthalmol 1989;86(3):221–223.
16. Glazer LC, Maguire A, Blumenkranz MS, et al. Improved surgical treatment of familial exudative vitreoretinopathy in children. Am J Ophthalmol 1995;120(4):471–479.
17. Shubert A, Tasman W. Familial exudative vitreoretinopathy: surgical intervention and visual acuity outcome. Graefes Arch Clin Exp Ophthalmol 1997;235(8):490–493.
18. Suzuki Y, Nishina S, Hiraoka M, et al. Congenital rotated macula with good vision and binocular function. Jpn J Ophthalmol 2009;53(5):452–454.

Biosketch

Sachiko Nishina, MD, PhD, received her medical degree in 1989 and completed residency in ophthalmology at Keio University School of Medicine, Japan. She became a fellow in pediatric ophthalmology and strabismus in National Children's Hospital, Japan in 1994. She received her PhD degree in 2001 from Keio University School of Medicine. She has practiced pediatric ophthalmology and strabismus at the Department of Ophthalmology, National Center for Child Health and Development, Japan since 2002. Her clinical and research interests include the management of pediatric ocular diseases and strabismus, pathology of pediatric ocular diseases, and embryology.

Development/Plasticity/Repair

Stress-Activated Protein Kinase MKK7 Regulates Axon Elongation in the Developing Cerebral Cortex

Tokiwa Yamasaki,[1,3] Hiroshi Kawasaki,[4,5] Satoko Arakawa,[2] Kimiko Shimizu,[6] Shigeomi Shimizu,[2] Orly Reiner,[7] Hideyuki Okano,[8] Sachiko Nishina,[9] Noriyuki Azuma,[9] Josef M. Penninger,[10] Toshiaki Katada,[3] and Hiroshi Nishina[1]

Departments of [1]Developmental and Regenerative Biology and [2]Pathological Cell Biology, Medical Research Institute, Tokyo Medical and Dental University, Bunkyo-ku, Tokyo 113-8510, Japan, [3]Department of Physiological Chemistry, Graduate School of Pharmaceutical Science, [4]Department of Molecular and Systems Neurobiology, Graduate School of Medicine, [5]Global COE Program "Comprehensive Center of Education and Research for Chemical Biology of the Diseases," and [6]Department of Biophysics and Biochemistry, Graduate School of Science, The University of Tokyo, Bunkyo-ku, Tokyo 113-0033, Japan, [7]Department of Molecular Genetics, Weizmann Institute of Science, Rehovot 76100, Israel, [8]Department of Physiology, School of Medicine, Keio University, Shinjuku-ku, Tokyo 160-8582, Japan, [9]Department of Ophthalmology, National Center for Child Health and Development, Setagaya-ku, Tokyo 157-8535, Japan, and [10]IMBA, Institute of Molecular Biotechnology of the Austrian Academy of Science, 1030 Vienna, Austria

The c-Jun NH^2-terminal protein kinase (JNK), which belongs to the mitogen-activated protein kinase family, plays important roles in a broad range of physiological processes. JNK is controlled by two upstream regulators, mitogen-activated protein kinase kinase (MKK) 7 and MKK4. To elucidate the physiological functions of MKK7, we used *Nestin-Cre* to generate a novel mouse model in which the *mkk7* gene was specifically deleted in the nervous system ($Mkk7^{flox/flox}$ *Nestin-Cre* mice). These mice were indistinguishable from their control littermates in gross appearance during embryogenesis but died immediately after birth without breathing. Histological examination showed that the mutants had severe defects in brain development, including enlarged ventricles, reduced striatum, and minimal axon tracts. Electron microscopy revealed abnormal accumulations of filamentous structures and autophagic vacuoles in $Mkk7^{flox/flox}$ *Nestin-Cre* brain. Further analysis showed that MKK7 deletion decreased numbers of TAG-1-expressing axons and delayed neuronal migration in the cerebrum. Neuronal differentiation was not altered. *In utero* electroporation studies showed that contralateral projection of axons by layer 2/3 neurons was impaired in the absence of MKK7. Moreover, MKK7 regulated axon elongation in a cell-autonomous manner *in vivo*, a finding confirmed *in vitro*. Finally, phosphorylation levels of JNK substrates, including c-Jun, neurofilament heavy chain, microtubule-associated protein 1B, and doublecortin, were reduced in $Mkk7^{flox/flox}$ *Nestin-Cre* brain. Our findings demonstrate that the phenotype of $Mkk7^{flox/flox}$ *Nestin-Cre* mice differs substantially from that of $Mkk4^{flox/flox}$ *Nestin-Cre* mice, and establish that MKK7-mediated regulation of JNK is uniquely critical for both axon elongation and radial migration in the developing brain.

Introduction

The activation of c-Jun NH^2-terminal protein kinase (JNK) results in the phosphorylation of numerous important substrates, including the AP-1 transcription factor c-Jun (Hibi et al., 1993) and various microtubule-associated proteins (MAPs) (Kawauchi et al., 2003; Gdalyahu et al., 2004), that control cellular processes such as cell growth, apoptosis, differentiation, migration, and transformation. JNK activation in response to environmental stresses, growth factors, hormones, and proinflammatory cytokines is triggered by mitogen-activated protein kinase (MAPK) kinase 4 (MKK4) and MKK7 (Davis, 2000; Chang and Karin, 2001; Asaoka and Nishina, 2010). While MKK4 activates both JNK and another MAPK, p38 (Enslen et al., 1998), MKK7 regulates only the JNK signaling cascade.

MKK7 modulates JNK signaling by interacting with scaffold proteins such as the JNK-interacting protein (JIP) 1, 2, or 3 or filamin A (Whitmarsh et al., 1998; Ito et al., 1999; Yasuda et al., 1999; Nakagawa et al., 2010). Previously, we reported that MKK7 has an essential role in liver development, in that *Mkk7* total knock-out mice die at E12.5–E13.5 with severely disorganized livers and reduced hepatoblast numbers (Wada et al., 2004). This study also revealed that hepatoblast proliferation depends on the MKK7-JNK-c-Jun pathway. However, the functions of MKK7 in other tissues remain unclear due to the early embryonic lethality of *Mkk7* total knock-out mice.

Several lines of evidence have established the importance of JNK signaling in the mammalian brain. First, $Jnk1^{-/-}$ mice display an abnormality in the maintenance of telencephalic commissures

Received March 3, 2011; revised Sept. 18, 2011; accepted Oct. 4, 2011.

Author contributions: T.Y., H.K., T.K., and H.N. designed research; T.Y., H.K., S.A., and S.S. performed research; T.Y., K.S., O.R., H.O., S.N., N.A., and J.M.P. contributed unpublished reagents/analytic tools; T.Y., H.K., S.A., S.S., H.O., and H.N. analyzed data; T.Y., H.K., and H.N. wrote the paper.

This work was supported in part by research grants from the Ministry of Education, Culture, Sports, Science, and Technology of Japan, the Ministry of Health, Labour, and Welfare of Japan, and the Japan Society for the Promotion of Science. We are grateful to numerous members of the Nishina, Kawasaki, and Katada laboratories for critical reading and helpful discussions. We also thank Dr. Syu-ichi Hirai (Yokohama City University, Kanagawa, Japan) for his generous and expert technical advice.

Correspondence should be addressed to Dr. Hiroshi Kawasaki, Department of Molecular and Systems Neurobiology, Graduate School of Medicine, The University of Tokyo, 7-3-1 Hongo, Bunkyo-ku, Tokyo 113-0033, Japan, E-mail address: kawasaki@m.u-tokyo.ac.jp; or Dr. Hiroshi Nishina, Department of Developmental and Regenerative Biology, Medical Research Institute, Tokyo Medical and Dental University, 1-5-45 Yushima, Bunkyo-ku, Tokyo 113-8510, Japan, E-mail address: nishina.dbio@mri.tmd.ac.jp.

DOI:10.1523/JNEUROSCI.1111-11.2011

 0270-6474/11/3116872-12$15.00/0

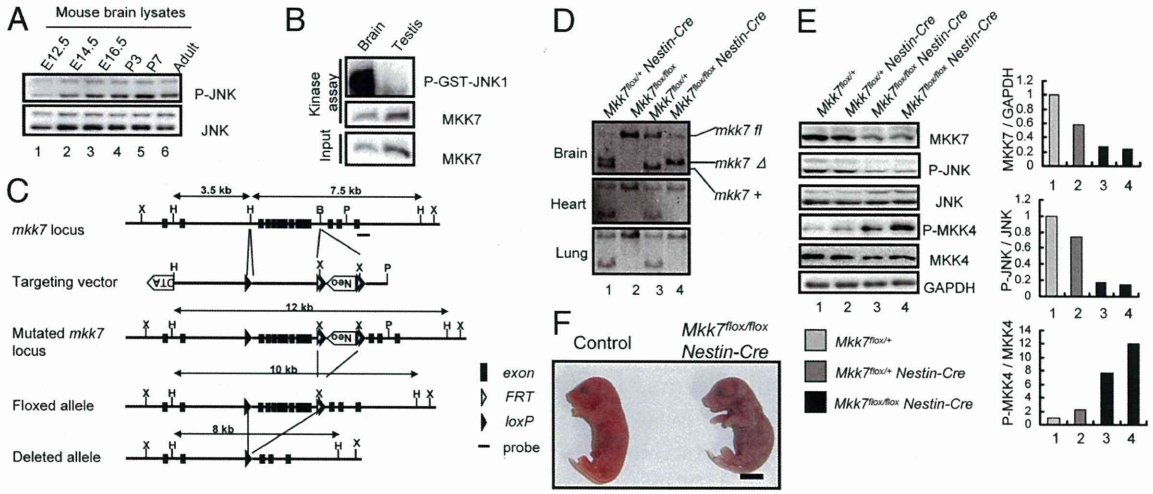

Figure 1. The MKK7-JNK signaling pathway is activated in the developing brain and essential for postnatal viability. ***A***, Analysis of JNK activity during mouse development. Extracts of brains from WT mice at the indicated stages of development were prepared and immunoblotted to detect JNK activity. ***B***, Analysis of MKK7 activity in WT adult mouse brain. MKK7 kinase activity was assayed as described in Materials and Methods. Testis, Negative control. ***C***, CNS-specific targeting of the murine *mkk7* gene. The genomic *mkk7* locus, the *mkk7* targeting vector, the predicted structure of the mutated *mkk7* locus, and the floxed and deleted *mkk7* alleles are depicted. Black boxes, *mkk7* exons; black arrowheads, loxP sites; white arrowheads, FRT sites; X, XbaI; H, HindIII; B, BamHI; P, PstI. The Neo and DTA cassettes and the probe used for Southern blotting are indicated. ***D***, Confirmation of MKK7 deletion. HindIII-restricted genomic DNA was prepared from mice of the indicated genotypes at E16.5 and subjected to Southern blotting with the probe in ***C***. ***E***, Suppression of JNK activity by MKK7 disruption in the CNS. Left, Extracts of brains of E18.5 embryos of the indicated genotypes were immunoblotted to detect the indicated proteins. Right, Normalized protein expression levels for MKK7/Gapdh, phospho-JNK/JNK, and phospho-MKK4/MKK4 in the extracts in the left panel were determined by densitometry and are shown in the histograms. ***F***, *Mkk7* disruption results in death immediately after caesarean section. Control and *Mkk7*$^{flox/flox}$ *Nestin-Cre* embryos were obtained by caesarean section at E18.5 and subjected to gross examination. All control mice started breathing (13/13), but most *Mkk7*$^{flox/flox}$ *Nestin-Cre* mice (9/10) did not and died immediately. Scale bar, 5 mm.

Table 1. MKK7 is critical for postnatal viability

		Number of embryos or newborns with genotype				
Stage	No. of litters	Total	*Mkk7*$^{flox/+}$	*Mkk7*$^{flox/flox}$	*Mkk7*$^{flox/+}$ *Nestin-Cre*	*Mkk7*$^{flox/flox}$ *Nestin-Cre*
E12.5	2	15	6	3	4	2
E14.5	6	46	10	11	17	8
E16.5	6	51	12	17	9	13
E18.5	7	54	14	9	14	17
P1	5	29	9	7	13	0

Mkk7$^{flox/+}$ *Nestin-Cre* mice were crossed with *Mkk7*$^{flox/flox}$ mice and the genotypes of embryos or neonates were determined by PCR at the indicated stages.

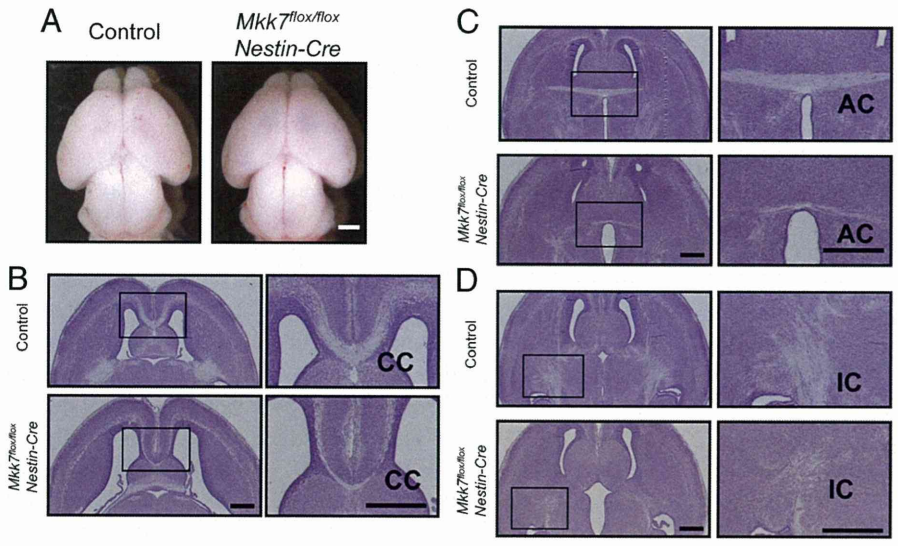

Figure 2. Lack of *Mkk7* causes abnormal brain development and reduced axon tracts in the cerebrum. ***A***, Gross appearance of whole brains of control and *Mkk7*$^{flox/flox}$ *Nestin-Cre* embryos at E18.5. Results are representative of embryos examined per genotype. Scale bar, 1 mm. ***B–D***, Histological analysis of brain defects in *Mkk7*$^{flox/flox}$ *Nestin-Cre* mice. Horizontal sections of the brains of control and *Mkk7*$^{flox/flox}$ *Nestin-Cre* embryos at E18.5 were stained with cresyl violet. Left, Forebrains with inset boxes indicating CC (***B***), AC (***C***), and IC (***D***) are shown. Scale bar, 500 μm. Right, Inset boxes in left panels are magnified. Scale bar, 500 μm.

(Chang et al., 2003) as well as altered dendritic architecture (Björkblom et al., 2005). Second, the dopaminergic neurons of both *Jnk2*$^{-/-}$ and *Jnk3*$^{-/-}$ mice resist MPTP-induced cell death (Hunot et al., 2004). Thirdly, *Jnk1/Jnk2* double mutant mice die at E11.5 with defective neural tube morphogenesis and reduced apoptosis in the hindbrain but increased apoptosis and caspase activation in the forebrain (Kuan et al., 1999; Sabapathy et al., 1999), showing that JNK signaling has both pro- and anti-apoptotic effects on the developing brain. Last, JNK signaling is involved in neuronal migration during brain development. Cortical neuronal migration was retarded by overexpression of a dominant-negative form of JNK (Kawauchi et al., 2003), and specific deletion of MKK4 in the CNS caused a delay in neuronal radial migration in the cerebral cortex as well as misalignment of Purkinje cells in the cerebellum (Wang et al., 2007). Together, these reports demonstrate that the proper control of JNK signaling is required for normal brain development; however, the specific role of MKK7 in this control has yet to be defined.

Here we report the generation of a novel mouse model, *Mkk7*$^{flox/flox}$ *Nestin-Cre* mice, in which the murine *mkk7* gene is specifically deleted in neural stem cells and postmitotic neurons. We found that *Mkk7*$^{flox/flox}$ *Nestin-Cre* mice display phenotypes different from those previously reported for *Mkk4*$^{flox/flox}$ *Nestin-Cre* mice, indicating that MKK7 has unique and crucial functions in the developing brain.

Materials and Methods

Animals. Mice carrying the *mkk7 flox* allele were described previously (Schramek et al., 2011). *Mkk7*$^{flox/flox}$ mice were crossed to

Nestin-Cre transgenic mice expressing Cre recombinase under the control of the mouse *nestin* promoter and the second intronic neural enhancer (Imai et al., 2006; Okada et al., 2006). The resulting control (*Mkk7*$^{flox/+}$, *Mkk7*$^{flox/flox}$ and *Mkk7*$^{flox/+}$ *Nestin-Cre*) and mutant (*Mkk7*$^{flox/flox}$ *Nestin-Cre*) mice were reared on a normal 12 h light/dark schedule. The day when a plug was observed in a female mouse was designated as embryonic day 0.5 (E0.5), and the day of birth was termed postnatal day 0 (P0). Mouse genotypes were determined by PCR and Southern blotting. For all experiments, only littermate mice from the same breeding were used. All procedures were performed in accordance with a protocol approved by the Tokyo Medical and Dental University Animal Care Committee.

In utero *electroporation.* *In utero* electroporation was performed as described previously (Saito, 2006; Tabata and Nakajima, 2008) with slight modifications. Briefly, pregnant mice were anesthetized with sodium pentobarbital and the uterine horns were exposed. Approximately 1–2 μl of DNA solution (1–2.5 mg/ml) was injected into the lateral ventricle of each embryonic brain using a pulled glass micropipette. Each embryo within its uterus was then placed between tweezer-type electrodes with a diameter of 5 mm (CUY650-P5; NEPA Gene). Square electric pulses (45 V, 50 ms) were passed five times at 1 s intervals using an electroporator (ECM830, BTX). Care was taken to quickly place embryos back into the abdominal cavity to avoid excessive temperature loss. The wall and skin of the abdominal cavity were sutured, and embryos were allowed to develop normally.

In vivo *neuronal migration.* Pregnant mice at E15.5 were injected intraperitoneally with bromodeoxyuridine (BrdU) (50 mg/kg of body weight). Embryos were dissected and fixed at E18.5 and brains were processed for paraffin sectioning. Deparaffinized and rehydrated 6 μm coronal sections were treated with 2N HCl at 37°C for 30 min and neutralized with 0.1% boric acid buffer, pH 8.5. After blocking in 2% skim milk in PBS containing 0.1% Triton X-100, sections were subjected to immunohistochemical analysis as described below.

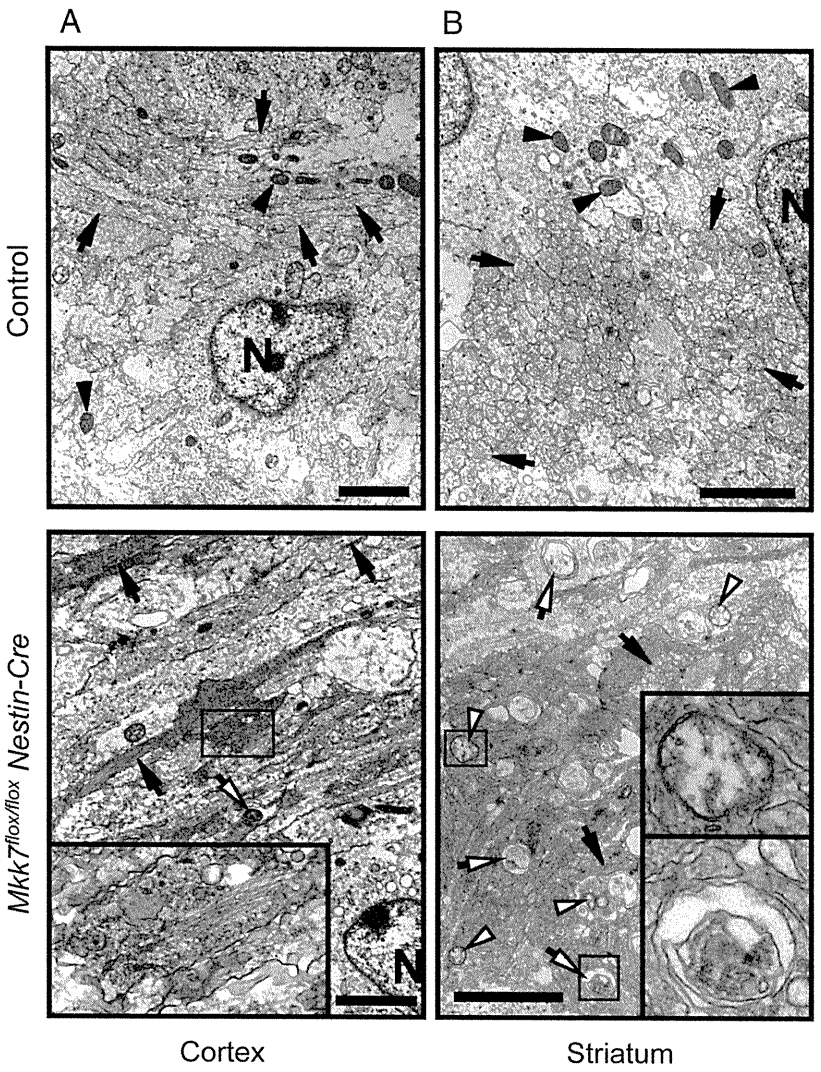

Figure 3. Loss of MKK7 causes accumulations of filamentous structures and autophagic vacuoles. Brains of control and *Mkk7*$^{flox/flox}$ *Nestin-Cre* embryos at E18.5 were analyzed by electron microscopy. The cortex (***A***) and striatum (***B***) are shown. Black arrows, Axons; black arrowheads, mitochondria; white arrows, autophagic vacuoles; white arrowheads, swollen mitochondria; N, nuclei. Inset boxes, ***A***, Accumulation of filamentous structures; ***B***, top, swollen mitochondrion; ***B***, bottom, autophagic vacuole. Scale bar, 2 μm.

Dissociation and culture of cortical neurons. At E16.5, cortices were dissected from *Mkk7*$^{flox/flox}$ *Nestin-Cre*, *Mkk7*$^{flox/flox}$, *Mkk7*$^{flox/+}$, or wild-type embryos that had been electroporated at E15.5. The dissected cortices were placed in culture and incubated for 20 min with papain solution plus DNase I at 37°C, followed by mechanical dissociation in dissociation medium (EBSS; Sigma-Aldrich). Cortical neurons were plated onto poly-L-lysine-coated coverslips, and maintained in Basal Medium Eagle (Invitrogen) containing 1 mM L-glutamine (Sigma), HBSS (Invitrogen), 25% (v/v) horse serum (Invitrogen), 6.6 mg/ml dextrose (Sigma), penicillin/streptomycin (Invitrogen), and 1 mM HEPES, pH 7.4 (Invitrogen). Cortical neuron cultures were maintained in 5% CO_2 at 37°C.

Immunoblotting. Immunoblotting was performed as previously described (Ura et al., 2007) with slight modifications. Proteins were extracted from tissues in TNE buffer [20 mM Tris-HCl, pH 7.4, 150 mM NaCl, 1 mM EDTA, 1 mM EGTA, 0.5% Nonidet P40, 5% (w/v) glycerol, 1 mM PMSF, 200 mM NaF, 200 μM Na_3VO_4, 10 μg/ml aprotinin]. Total extracts were clarified by centrifugation (20,000 × *g* for 10 min at 4°C) and soluble proteins in the supernatants were quantified using the BCA Protein Assay Kit (PIERCE). Protein extracts were fractionated by SDS/PAGE and transferred to a PVDF membrane, which was incubated in blocking solution (2% skim milk in TBS) for 1 h. The blocked membrane was incubated overnight in TBS containing 5% BSA plus antibodies recognizing phospho-JNK (Cell Signaling Technology), JNK1 (46 kDa and 55 kDa splicing variants; Santa Cruz Biotechnology), MKK7 (Cell Signaling Technology), GAPDH (Millipore Bioscience Research Reagents), phospho-MKK4 (Cell Signaling Technology), MKK4 (Santa Cruz Biotechnology), phospho-DCX (Gdalyahu et al., 2004), DCX (Gdalyahu et al., 2004), phospho-neurofilament heavy chain (Covance), phospho-MAP1B (Covance), MAP1B (Sigma), or tubulin (Invitrogen). The membrane was then washed in TBS/Tween 20 (0.05%), incubated for 1 h with anti-mouse/rabbit horseradish peroxidase-conjugated antibodies (Jackson ImmunoResearch Laboratory), and washed three times in TBS/Tween 20. Proteins were visualized using Immobilon-HRP (Millipore) or the SuperSignal West Femto Kit (Pierce) and Chemi-Doc XRS (Bio-Rad).

In vitro *kinase assay.* Assay of MKK7 activity was as described previously (Nakagawa et al., 2010). Endogenous MKK7 proteins were immunoprecipitated with anti-MKK7 (KN-004) monoclonal antibody (Wada et al., 2001). Immunocomplexes were washed three times with lysis buffer and three times with kinase reaction buffer, which consisted of 10 mM $MgCl_2$, 50 mM Tris-HCl, pH 7.5, and 1 mM EGTA. MKK7 activity on beads was measured using an *in vitro* MAPK kinase assay using 100 μM ATP and GST-JNK1 as the substrate. Reactions were terminated after 30

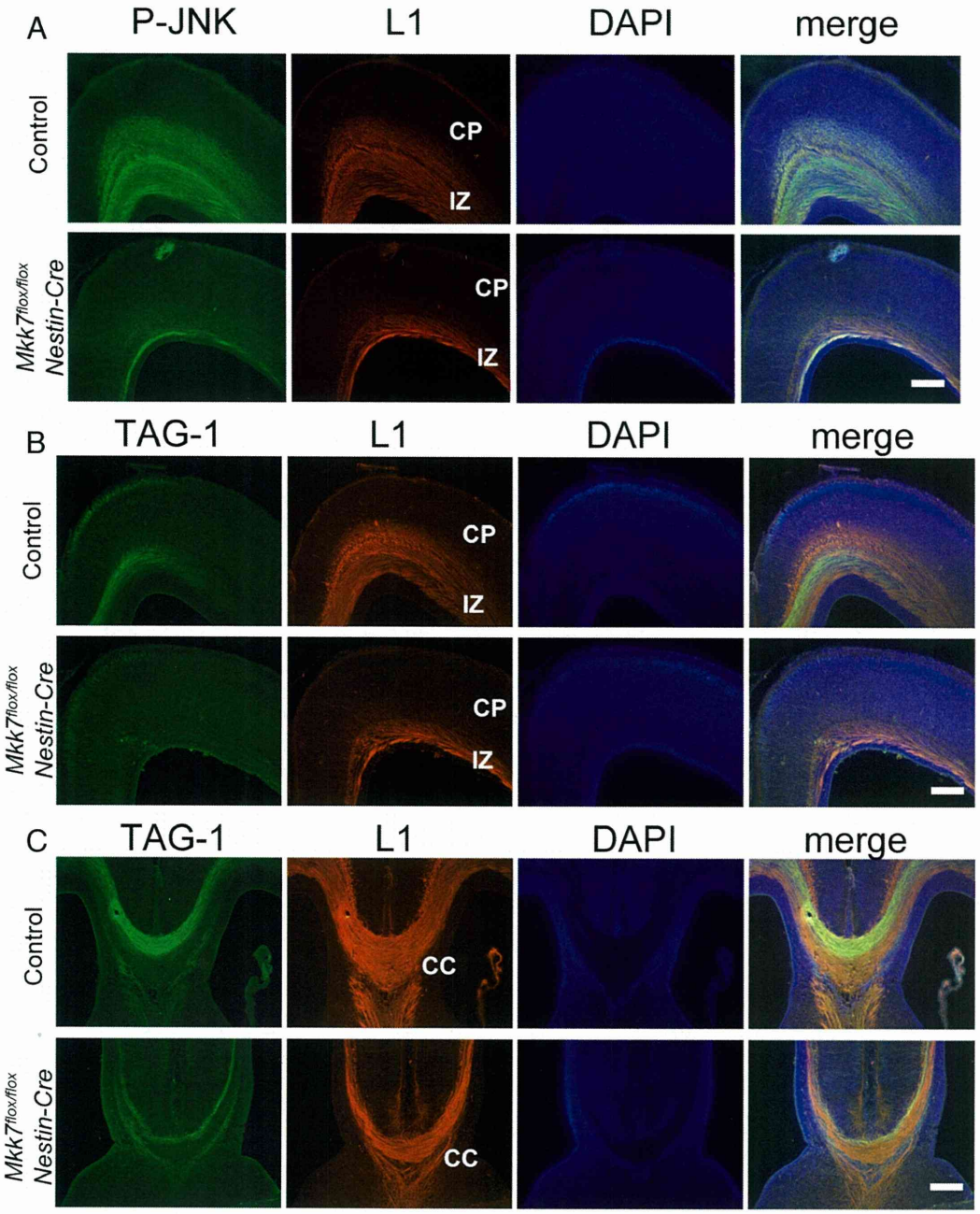

Figure 4. Axonal defects in the cortex and corpus callosum of *Mkk7*$^{flox/flox}$ *Nestin-Cre* mice. ***A***, Suppression of JNK phosphorylation in axons. Coronal sections of the cortex in control and *Mkk7*$^{flox/flox}$ *Nestin-Cre* embryos at E18.5 were immunostained with anti-phospho-JNK and anti-L1 antibodies. DAPI staining was used to visualize nuclei. CP, Cortical plate; IZ, intermediate zone. ***B***, ***C***, Coronal sections of the cortex (***B***) and the CC (***C***) in control and *Mkk7*$^{flox/flox}$ *Nestin-Cre* embryos at E18.5 were immunostained with anti-TAG-1 and anti-L1 antibodies as for ***A***. Scale bar: ***A–C***, 200 μm.

min at 30°C by the addition of 4× SDS gel sample buffer. The reaction product was detected using anti-phospho-JNK antibody.

Nissl staining. Nissl staining was performed as described previously (Toda et al., 2008) with slight modifications. Brains were fixed at E18.5 and processed for paraffin sectioning. Deparaffinized and rehydrated 6 μm horizontal sections were subjected to Nissl staining with 0.2% cresyl violet.

Immunostaining. Immunohistochemistry was performed as described previously (Kawasaki et al., 2000). For embryos, brains were isolated and fixed overnight in 4% paraformaldehyde. For postnatal mice, the animals were deeply anesthetized with pentobarbital and transcardially perfused with 4% paraformaldehyde. Fixed tissues were cryoprotected by overnight immersion in 30% sucrose, followed by embedding in OCT compound. Sections of 14 μm thickness were attached to glass slides, whereas sections of 50 μm thickness were floated on PBS. For cultures of dissociated neurons, cells were fixed by incubation in 4% paraformaldehyde for 5 min at 37°C.

For immunostaining, tissue sections and isolated cells were permeabilized with 0.1–0.5% Triton X-100 in PBS and incubated overnight with primary antibodies, including those recognizing phospho-JNK (Cell Signaling Technology), TAG-1 (DSHB), L1 (Millipore Bioscience Research Reagents), cleaved caspase-3 (PharMingen), β-tubulin III (Covance), Brn2 (Santa Cruz Biotechnology), Satb2 (Abcam), Ctip2 (Abcam), Foxp2 (Abcam), Tbr2 (Abcam), or GFP or RFP (both from MBL). Immunostained tissues and cells were then incubated with Alexa488- and/or Cy3-conjugated secondary antibodies and 1 μg/ml Hoechst 33342, followed by washing and mounting. Epifluorescent microscopy was performed using an Axioimager A1 microscope (Carl Zeiss) and BZ9000 (Keyence). Confocal microscopy was performed using an LSM510 microscope (Carl Zeiss).

Electron microscopy. Tissues were fixed by immersion first in 1.5% paraformaldehyde plus 3% glutaraldehyde in 0.1 M phosphate buffer, pH 7.3, and then in an aqueous solution of 1% OsO_4. Fixed samples were

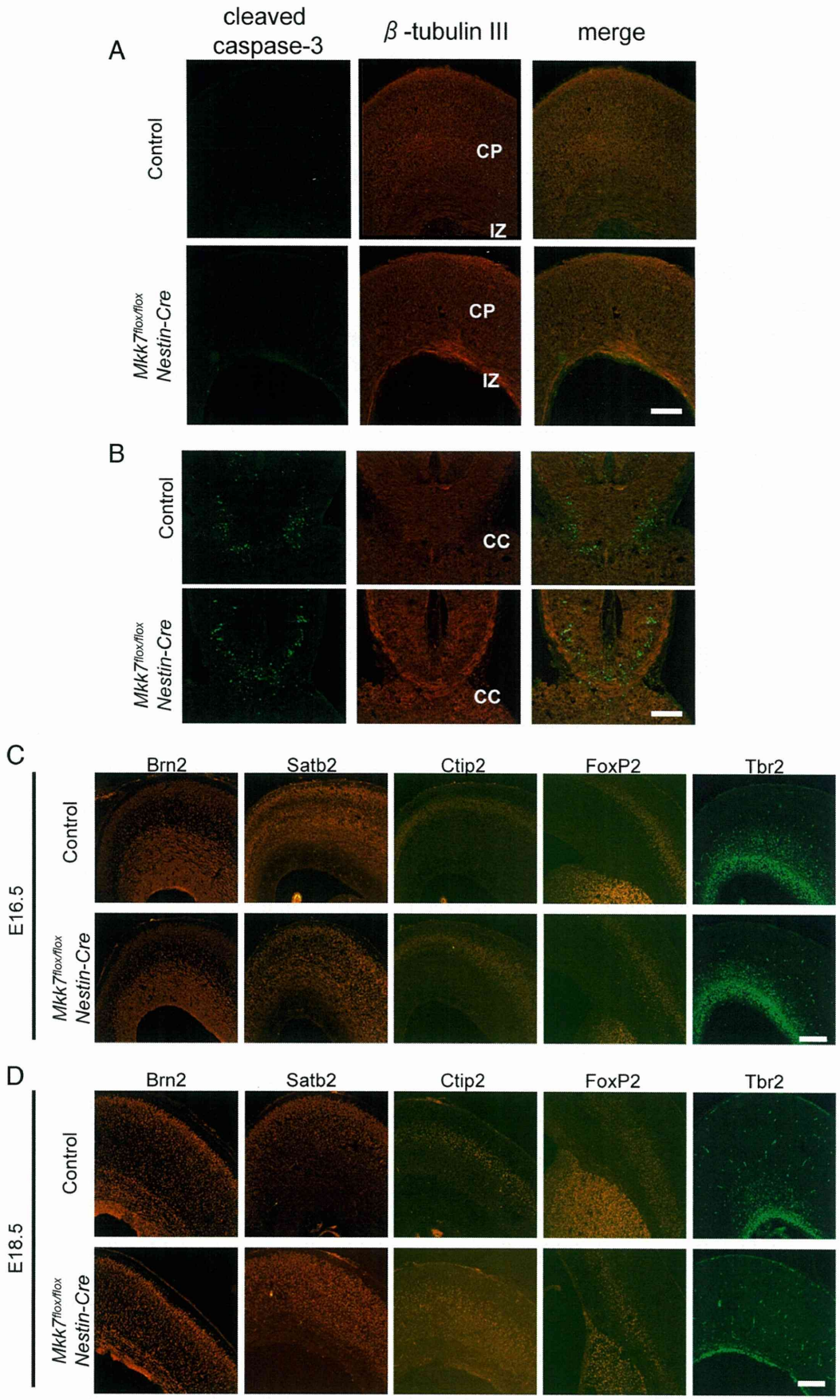

Figure 5. Loss of MKK7 does not influence apoptosis or neuronal differentiation in the brain. ***A***, ***B***, Coronal sections of cortex (***A***) and CC (***B***) in control and *Mkk7*$^{flox/flox}$ *Nestin-Cre* embryos at E18.5 were immunostained with anti-cleaved caspase-3 and anti-β-tubulin III antibodies. ***C***, ***D***, Coronal sections of the cortex in control and *Mkk7*$^{flox/flox}$ *Nestin-Cre* embryos at E16.5 (***C***) or E18.5 (***D***) were immunostained with antibodies recognizing the neuronal markers Brn2, Satb2, Ctip2, Foxp2, or Tbr2. Scale bar, 200 μm.